NORTHERN CALIFORNIA GEOLOGICAL SOCIETY

Geologic Field Trip Guide to Angel Island San Francisco Bay, California

September 28, 2024

Field Trip Leaders: Tom MacKinnon, Don Medwedeff, Bill Motzer, Will Schweller and Greg Bartow



Google Earth image of Angel Island with approximate field trip route.

Introduction

This field trip is an outgrowth of field trips led mainly by Professor Christie Rowe and her student Dr. Meghomita Das from McGill University. Much of the material in this guidebook was provided by Dr. Das and comes from her PhD Thesis. Prof. Rowe and Dr. Das separately received grants from the NCGS to support their respective thesis studies.

Geologic Introduction and Overview

Angel Island is a prominent feature in the northern part of San Francisco Bay, California. Exposures on Angel Island represent the three basic elements of subduction zones: oceanic mantle, oceanic crust, and overlying deep water sediments. Metamorphic petrology and detrital zircon dating indicate that these sedimentary rocks represent a range of burial depths from ~10 to >25 km and depositional ages from 110 to 97 Ma. Finally, the field relationship among the various units requires a complex, if not fully understood, burial and exhumation history. This trip provides an opportunity to directly observe some of these elements and to discuss others.

Observations (in stratigraphic order from top to bottom):

- Graywacke sandstone metamorphosed to a sub-blueschist facies - Stop 6
- Graywacke sandstone metamorphosed to blueschist facies - Stops 1, 2, 4, & 5
- Bedded red chert - Stop 7
- Pillow basalt metamorphosed to blueschist facies - Stop 4
- Serpentinite (hydrated mantle peridotite) - Stops 3 and 4

Discussion Points:

- Angel Island can be divided structurally into four domains:
    - Low-metamorphic-grade graywackes in the footwall of the Quarry Point Thrust
    - Blueschist-metamorphic-grade (and interleaved lower-grade) graywackes in the hanging-wall of the Quarry Point Thrust
    - A 50 - 250 m wide shear zone of serpentinite, representing hydrated mantle peridotite either forming or intruding along a major fault zone.
    - Blueschist-metamorphic-grade basalt and gabbro west of the serpentinite shear zone.

- In the Franciscan Complex outcrop domain north of the Bay Area, blueschist facies rocks generally occur in the easternmost series of exposures. Here they are exposed within the less metamorphosed "Central Belt". Why might the two areas have developed differently?

- More specifically, what mechanisms were responsible for the burial, juxtaposition, and subsequent exhumation of these diverse rock suites?

Field Trip Logistics Overview

Field trip participants will arrive at Angel Island via the Angel Island Ferry that departs from Tiburon or San Francisco. Participants should buy their round-trip tickets online prior to the trip to insure they have a space on the ferry and to save time. The ferry from Tiburon to Angel Island takes about 10 minutes and arrives at the ferry dock on the north side of the island. The fee for the ferry is NOT included in the field trip cost.

Once we have disembarked from the ferry, we will use the Angel Island Tram to transit to the south end of the island and our first stop. From there, we will walk along the paved perimeter road west and then north, eventually coming back to the ferry landing. The distance along the perimeter road is approximately 4 miles, not including two side trips to Perles Beach and Kayak Beach. These two locations require fairly steep hikes down to the shoreline and back up to perimeter road along trails that can have difficult sections. Lugged hiking shoes or boots and hiking poles are strongly recommended.

The entire trip from arriving at the ferry landing to departing from the ferry landing will take about 6 hours. We will have lunch (bring your own) at one of many scenic overviews that have benches and picnic tables. Restrooms are available at the ferry landing and Stop 4. Water is available at only a few points along the trail, so be sure to bring a good supply.

Cultural History of Angel Island. (From Wikipedia)

Until about ten thousand years ago, Angel Island was connected to the mainland because of lower sea levels. It was cut off by the rise in sea levels at the end of the last ice age. From about two thousand years ago the island was a fishing and hunting site for Coast Miwok Native Americans. In 1775, the Spanish naval vessel San Carlos made the first European entry to the San Francisco Bay under the command of Juan de Ayala. Ayala anchored off Angel Island and gave it its modern name (Isla de los Ángeles). The bay where he anchored is now known as Ayala Cove. Up until 1850 the island was used as a source of lumber and for cattle ranching. In 1850, President Millard Fillmore declared Angel Island a military reserve and during the Civil War, the island was fortified to defend San Francisco Bay from potential attack by Confederate forces.

Angel Island continued to be an active military installation through World War II. In the later 19th century, the army designated the entire island as "Fort McDowell" and developed further facilities there, including what is now called the East Garrison or Fort McDowell. A quarantine station was opened in Ayala Cove (which at the time was known as Hospital Cove) in 1891. During the Spanish–American War the island served as a discharge depot for returning troops. It continued to serve as a transit station throughout the first half of the 20th century, with troops engaged in World War II embarking and returning there. From 1910 to 1940, Angel Island served as an immigration station. During this time, an estimated half a million people, a majority from China, Japan and other Asian countries, passed through Angel Island.

Tectonic Setting and Geology

The Franciscan Complex is part of a belt of largely Cretaceous rocks of accretionary origin that rim the circum-Pacific. Other well-known examples include: the Shimanto Belt in Japan, the Kodiak accretionary complex in Alaska and the Torlesse terrane in New Zealand. All of these accretionary complexes are composed primarily of graywacke sandstone and argillite with lesser volcanics, serpentinite, and chert. In addition, they all generally display a landward-thickening wedge geometry and a pattern of decreasing age and metamorphism oceanward. These first-order observations led to the consensus that the belts grow by addition of material above the subduction "megathrust" at their oceanward edges. At blueschist facies depth, the term used is **underplating**. At the subduction plate interface, rock is sliced off along zones of relatively weakness, which may be discreet faults or complex shear zones (Platt, 1986, Tewksbury et al, 2021).

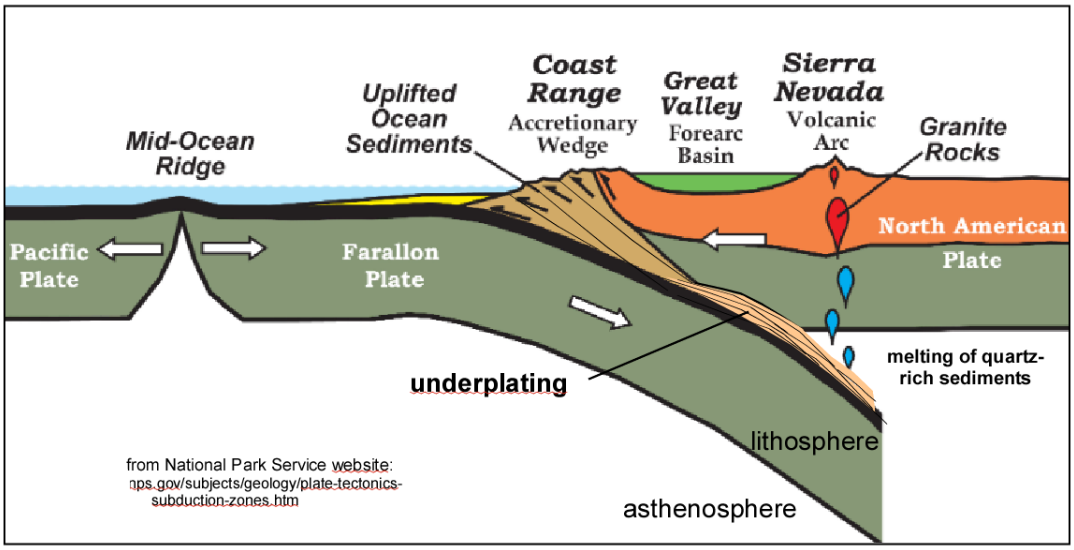


***Figure 1**: Generalized model for subduction and accretion on the western margin of North America.*

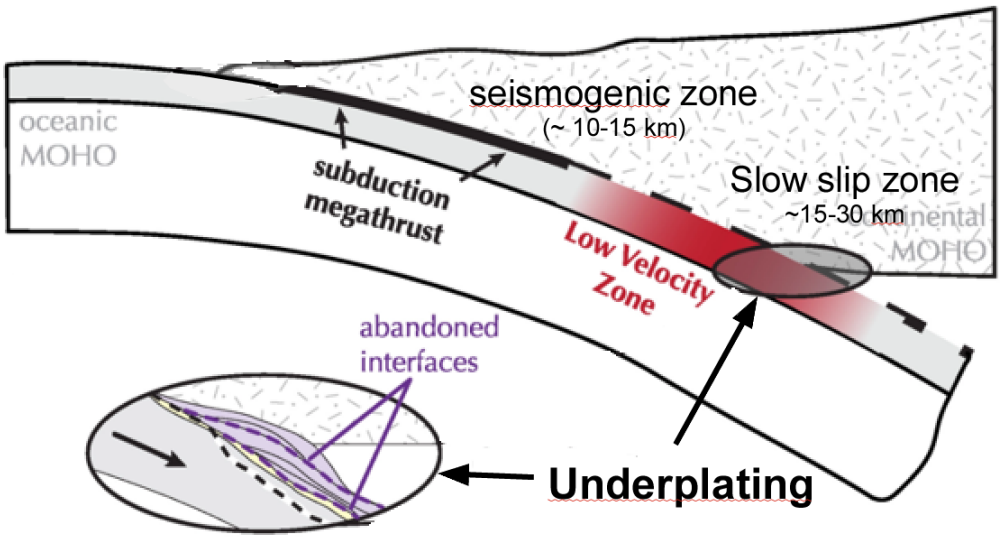


***Figure 2**: Cross-section model of subduction zone underplating (Modified from Tewksbury et al., 2021)*

Subduction zones can be divided into a seismogenic zone, which is locked and where large earthquakes occur, and a slow slip or low velocity zone which is lubricated and is where underplating occurs. The slow slip zone is characterized by slow earthquakes and fluid movement which may last for hours or days. Underplating appears to be associated with "Slow" earthquakes.

Recognizing underplated slices (e.g., Agard et al 2018) is key to understanding the process. In the Franciscan, there are many examples that have or can be interpreted as underplated slices. The best known are the Marin headlands (Wahrhaftig 1984a; Regalla et al., 2018; Raymond et al., 2019), and Pacheco Pass (Kimura et al., 1996) where duplexed graywacke, volcanics, and chert were mapped in several fault-bounded units measuring no more than 500 m thick.

Subduction zone temperature, pressure, and metamorphic facies

Generally, in the earth temperature increases with depth. Since pressure increases with the thickness of the over burden, high temperature regimes normally coincide with high pressure regimes. As shown by the numerical modelling of Peacock et al. (2020) (Fig. 3), rapid subduction of relatively cold oceanic crust and mantle results in anomalous high-pressure / low-temperature regimes.

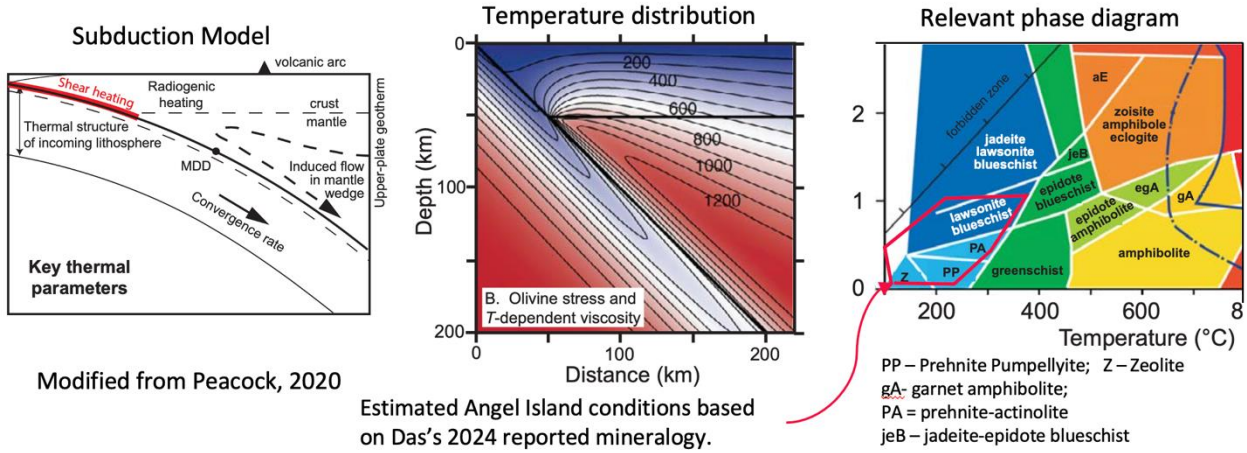


***Figure 3**: Subduction thermal model and corresponding metamorphic facies stabilities fields. (Modified from Peacock, 2020). Note that rapid subduction of relatively cold oceanic crust and mantle result in anomalous high-pressure / low-temperature regimes. The stability field indicated by mineral assemblages reported by Das (2024) are highlighted in the red polygon.*

Three Belts of Franciscan

In Northern California, the Franciscan has been divided into three belts, the Eastern, Central, and Coastal belts, based on a combination of geographic, lithologic and metamorphic criteria (Berkland *et al.* 1972}. This simple threefold subdivision seems to work reasonably well in Northern California, with caveats as outlined by Raymond (2017), but is particularly problematic further in the Bay Area where the belts display along strike variations in geology coupled with disruption by Tertiary strike-slip faults (Wakabayashi 2015; Raymond 2017; Ernst 2017).

Belt	**Age**	**Grade**	**Burial Depth**
Eastern	mostly Early Cretaceous	Blueschist	~15-30 km
Central	mostly Late Cretaceous	Prehnite Pump.	~10-20 km
Coastal	Late Cret. To Miocene	Zeolite	<10 km

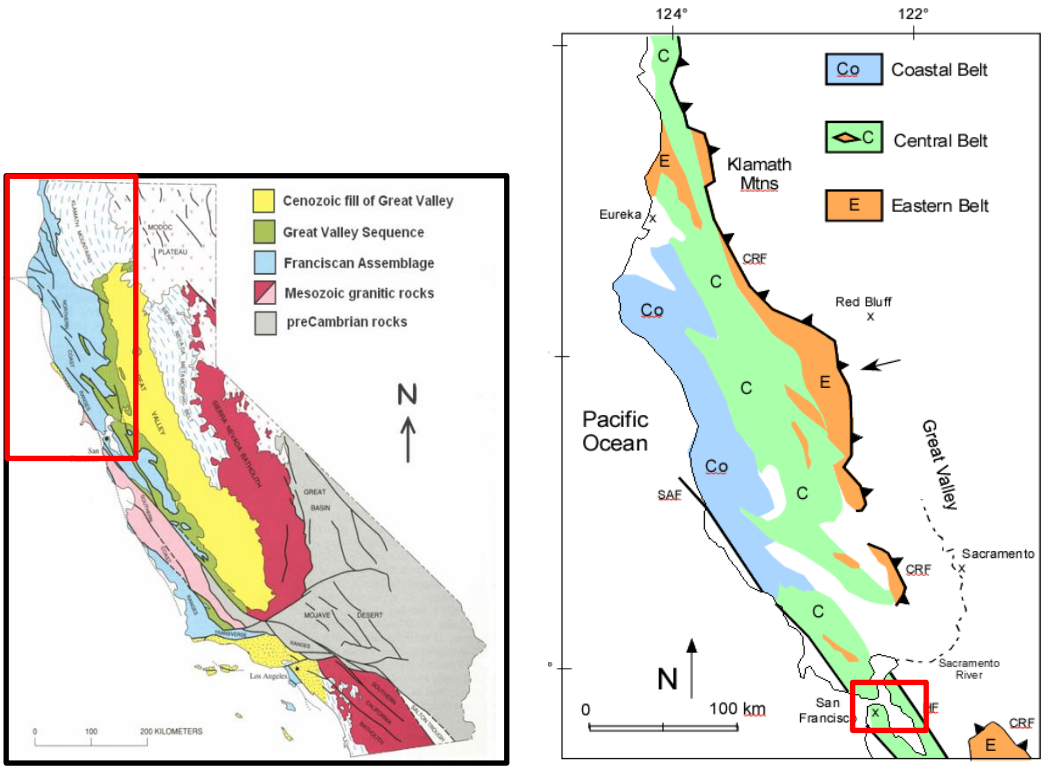


***Figure 4**: Maps of generalized California geology (left, from Irwin, 1990). and the three Franciscan belts in Northern California (right. From Raymond 2017 and Wakabayashi, 2017),*

In the Franciscan, rocks are commonly viewed as 1. coherent or broken formation or 2. mélange or dismembered formation (Fig. 5). "Coherent" units or Broken formation are broadly defined as strata that function as a rock stratigraphic unit. These units are rarely over 1 km thick and are typically thinner. Melange/dismembered formation consists of blocks of rock floating in a mudstone or serpentine matrix. Mélange contains exotic blocks whereas dismembered formation does not. Their origin is generally attributed to sedimentary (olistostromal) or tectonic processes with many examples showing features of both. In the Franciscan, broken formation/coherent units are much more common than mélange. Very roughly, mélange may comprise 10 to 20% of the Franciscan and most of this is in the Central Belt.

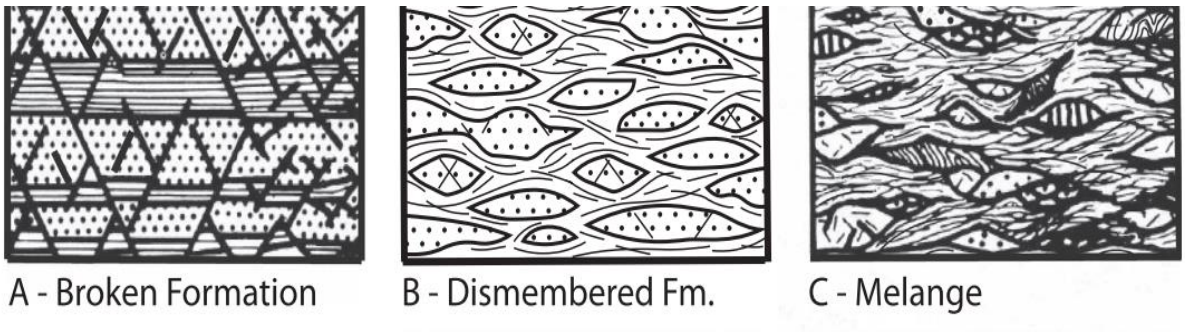


Figure 5: *See text above for description. from Raymond (2019)*

Franciscan Terranes and Geologic Mapping

A terrane is defined as **a fault-bounded block containing rocks that have a distinct geologic history compared with contiguous blocks**. Terranes were popularized by Clark Blake, David Jones and David Howell, all at the USGS in Menlo Park, in the early 1980's. Franciscan terranes in the Bay area commonly consist of several outcrops separated by areas of no exposure. Correlation is generally based on similar lithology, a general NW-SE outcrop trend and imprecise dating, such as zircon dating. Though most terranes shown in Figure 6 are probably closely related in time and space, there remain uncertainties.

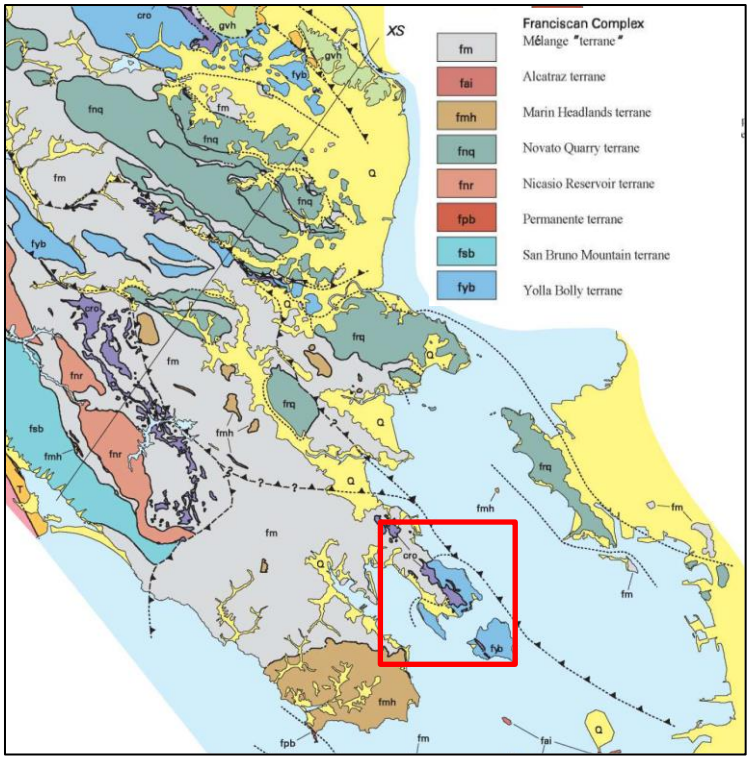
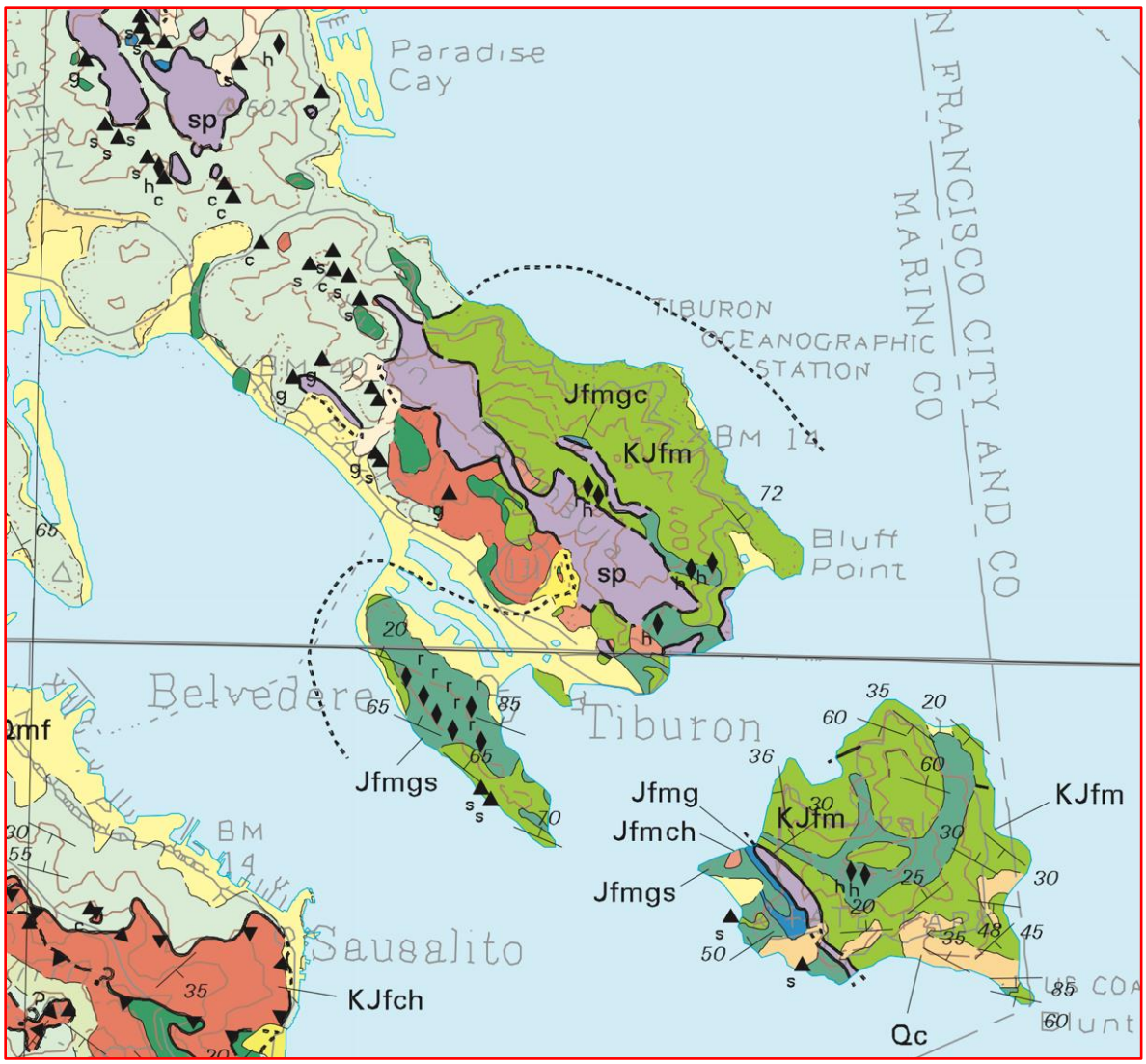


Figure 6. *Mapped terranes in Angel Island and nearby parts of San Francisco Bay. (Blake et al., 2000). Red box corresponds to the approximate area of Figure 7.*



KJfm	Metamorphic rocks (Cretaceous and Jurassic)	Jfmgc	Metagreenstone and metachert (Jurassic)
KJfch	Chert (Cretaceous and Jurassic)	Jfgs	Greenstone (Jurassic)
KJfgc	Greenstone and chert (Cretaceous and Jurassic)	Jfmg	Metamorphic rocks (Jurassic)
Jfg	Greenstone (Jurassic)	Jspm	Massive serpentinite (Jurassic)
Jfmgs	Metagreenstone (Jurassic)	sp	Serpentinite (Jurassic)
Jfmch	Metachert (Jurassic)	sc	Silica-carbonate rock (Jurassic)
		fsr	Mélange

Figure 7: *Mapped geology of Angel Island and nearby parts of San Francisco Bay. (Blake et al., 2000)*

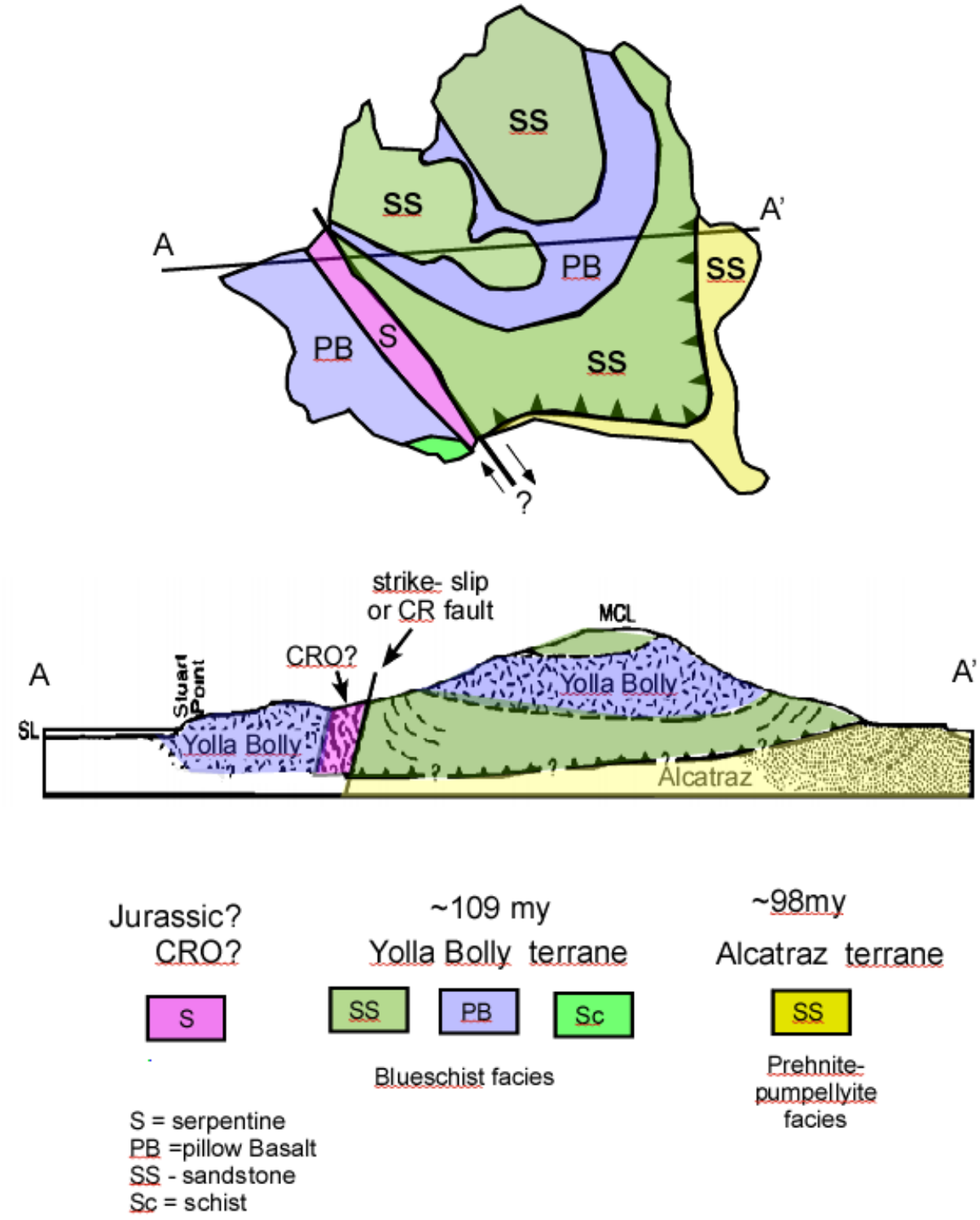


Figure 8. *Map and east-west cross section showing a low-angle fault separating the Yolla Bolly in the hanging-wall from the Alcatraz terrane in the footwall. Das (2024) denotes this fault as the Quarry Point thrust. From Konigsmark, T., 1998, after Wharhaftig 1984b.*

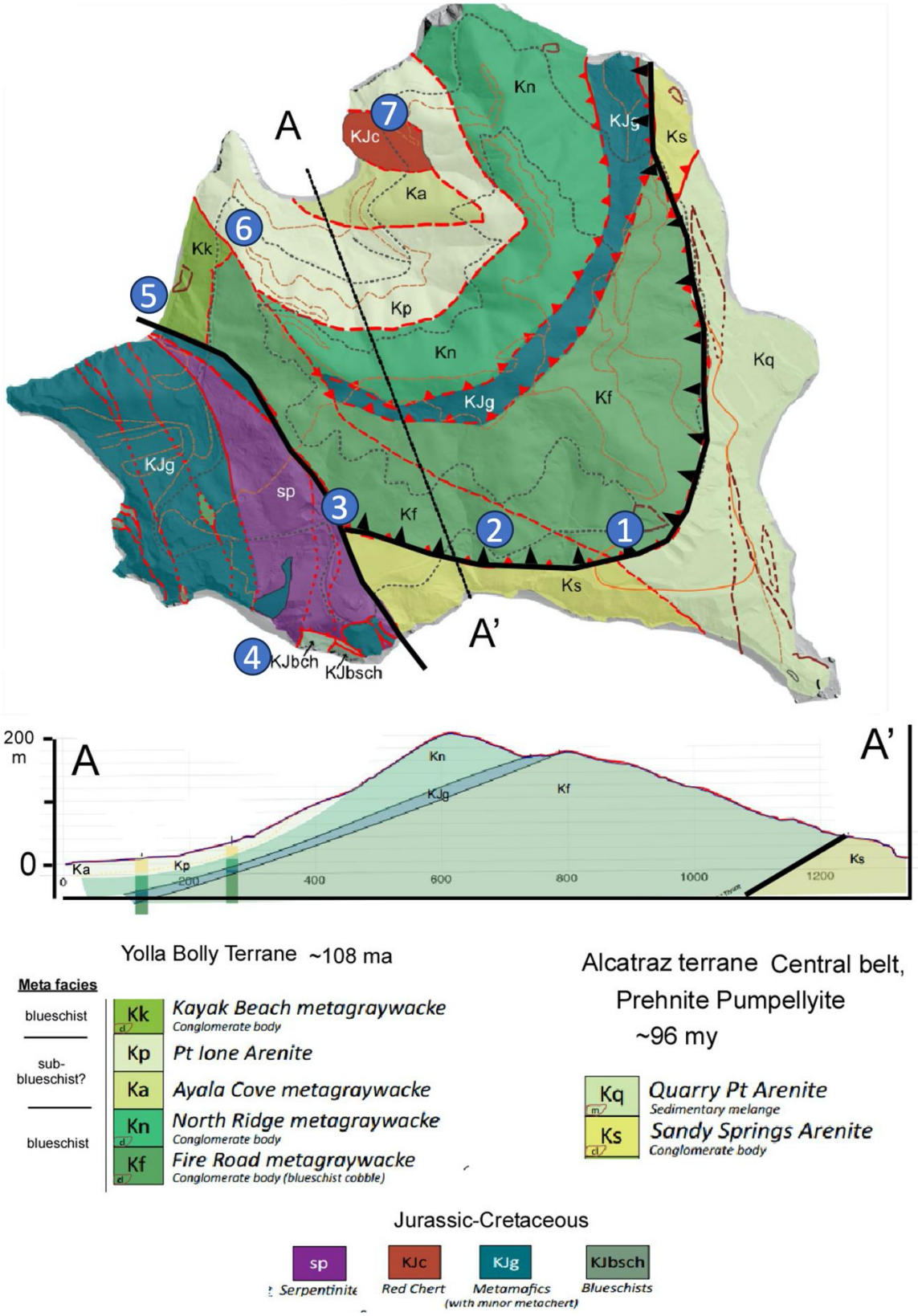


Figure 9: *Geologic map of Angel Island (Das, 2024) and cross section showing what can be interpreted as several underplated slices.*

Structural Analysis

Das (2024) provides observations demonstrating that Angel Island deviates from the oceanward decrease in metamorphic grade and deformation described above for Northern California Coast Ranges.



***Figure 10. Comparative sandstone fabric and metamorphic grade**. Field appearances of the metaclastics that highlight the mesoscale characteristics of each unit with their respective metamorphic grade. The units are arranged based on their relative positions with respect to Quarry Point Thrust. Dashed red lines indicates undifferentiated fault contact between the units. A thrust fault separates the Sandy Springs arenite in the hanging wall from the Quarry Point arenite in the footwall. From Das (2024)*

From mineralogy and rock fabric, Das (2024) interpreted that the blueschist units (North Ridge, Fire Road, Kayak Beach and interleaved meta-basalt) formed at temperatures of 300-400 C and pressures of 750-1,140 MPa. In contrast, Das (2024) identified the Quarry Point, Point Ione, Sandy Springs and Ayala Cove units as sub-blueschist, because they lack Jadeite or lawsonite.

Das (2024) notes that “the lower-grade to sub-metamorphic units (Sandy Springs and Quarry Point/Blunt Point) have a ~10 My younger depositional age with a distinct detrital zircon age spectrum. This juxtaposition could only have taken place shallower than the peak depth of the sub-metamorphic units, potentially at very shallow (diagenetic) depths, requiring the blueschists to have been substantially exhumed by this time. We suggest that intra-wedge shortening in the upper plate of the Farallon subduction zone is a reasonable setting for this juxtaposition.

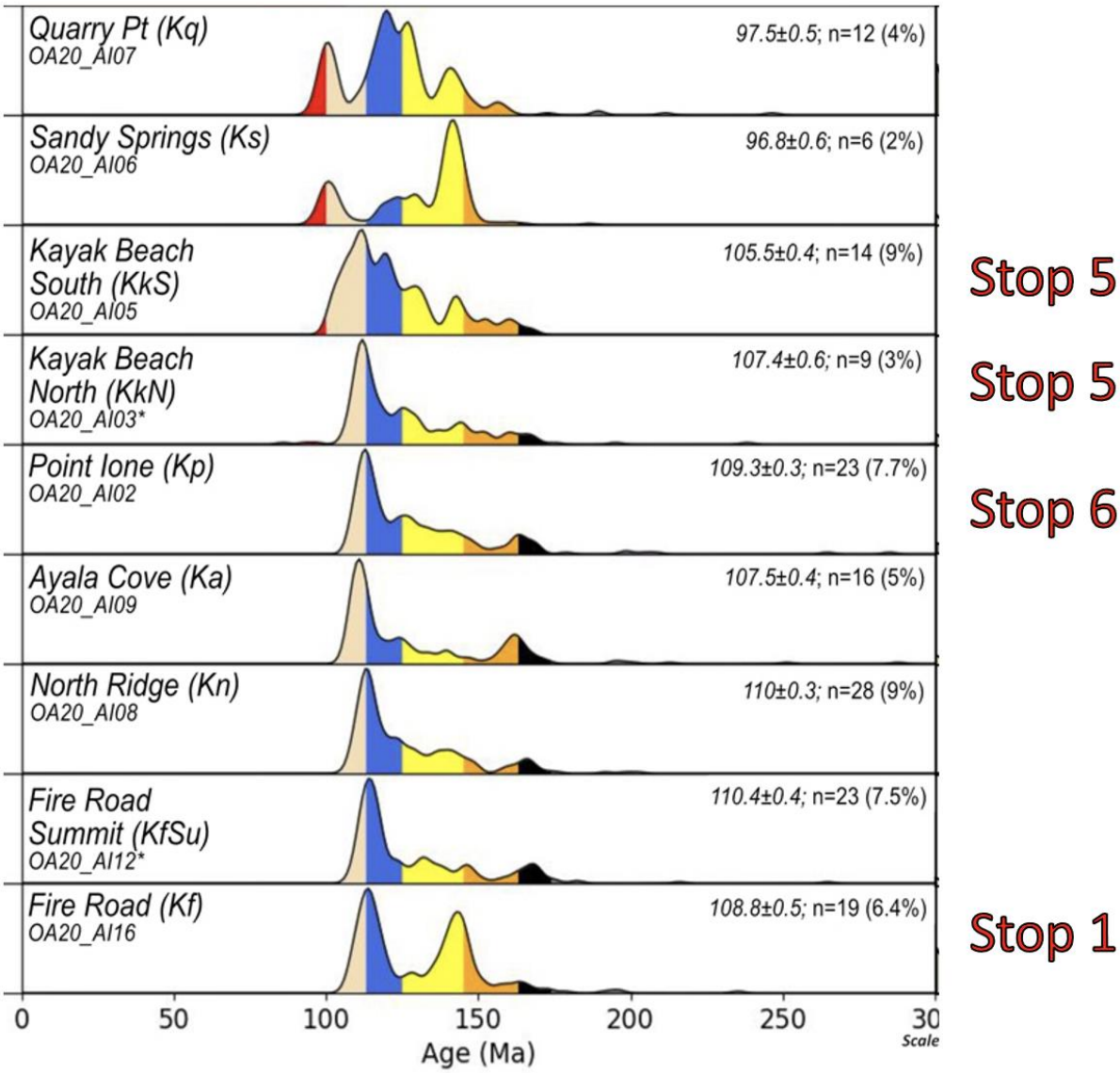
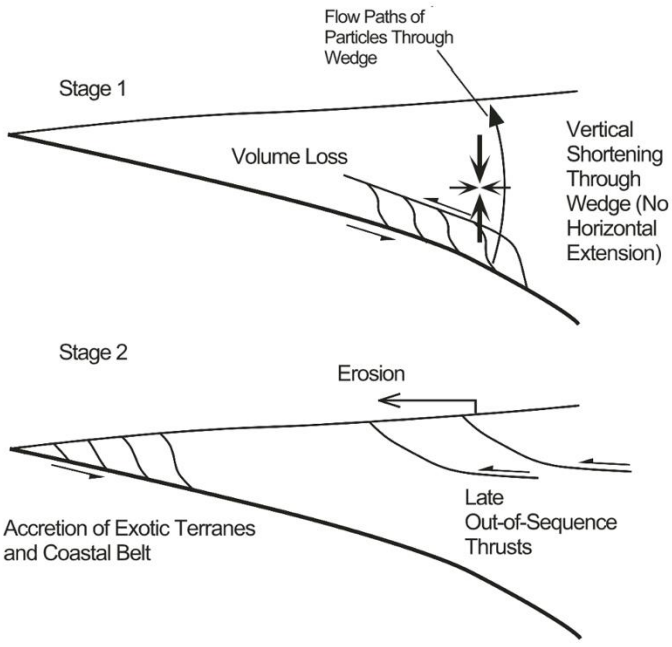


Figure 11. *Cumulative Distribution Plot (CDP) and Kernel Density Estimates (KDE) showing the detrital zircon U-Pb age date for the 9 metaclastic samples from Angel Island (Plot produced with Detrital Py software of Sharman et al. (2018)). In the legend of the CDP, N= (total number of ages reported) with a key in the left showing the age bins for the KDE. Samples are arranged according to stratigraphic succession of youngest to oldest. From Das (2024).*

Das (2024) concluded the following, based on observations of the structural evolution in the metaclastics of Angel Island and their ages as they accreted to the Franciscan Complex:

1. The metaclastics show a progressive intensification of their structural fabric that is broadly correlated to the development of metamorphic indicator minerals as the sediments get buried deeper and accreted onto the overriding plate. Metamorphic phyllosilicates replacing feldspar and lithic grains promote foliation development. Blueschist indicator minerals are associated with the most intense fabrics.
2. The maximum depositional ages for the blueschist- and sub-blueschist units (Angel Island; 105-110 Ma) and diagenetic-grade units (97-98 Ma) match well with the ages derived from other similar metasedimentary terranes in the Franciscan Complex. However, the detrital zircon spectra, when considered with grade and lithology, do not support correlating the units below the Quarry Point thrust with any other specific Bay Area clastic units.
3. The subduction, underplating, and subsequent structural juxtaposition of metaclastic units of different metamorphic grade but similar depositional ages suggests that ~105 - <95 Ma was a period of wedge thickening and shortening in the Farallon subduction zone.

Das' (2024) analysis for structural history at Angel Island in particular is broadly consistent with the two-stage process for uplift and exhumation of the Franciscan complex proposed by Ring (2008).



In stage 1, subducted rocks are attached to the base of the wedge via underplating and then rise vertically via pressure-solution induced shortening during continued underplating.

In stage 2, uplifted and cooled rocks are exhumed by out of sequence thrusts. Such out of sequence thrusts might explain the complex juxtaposition of metamorphic facies described by Das (2024).

Figure 12. *Two-stage process for uplift and exhumation of the Franciscan Complex (Ring, 2008).*

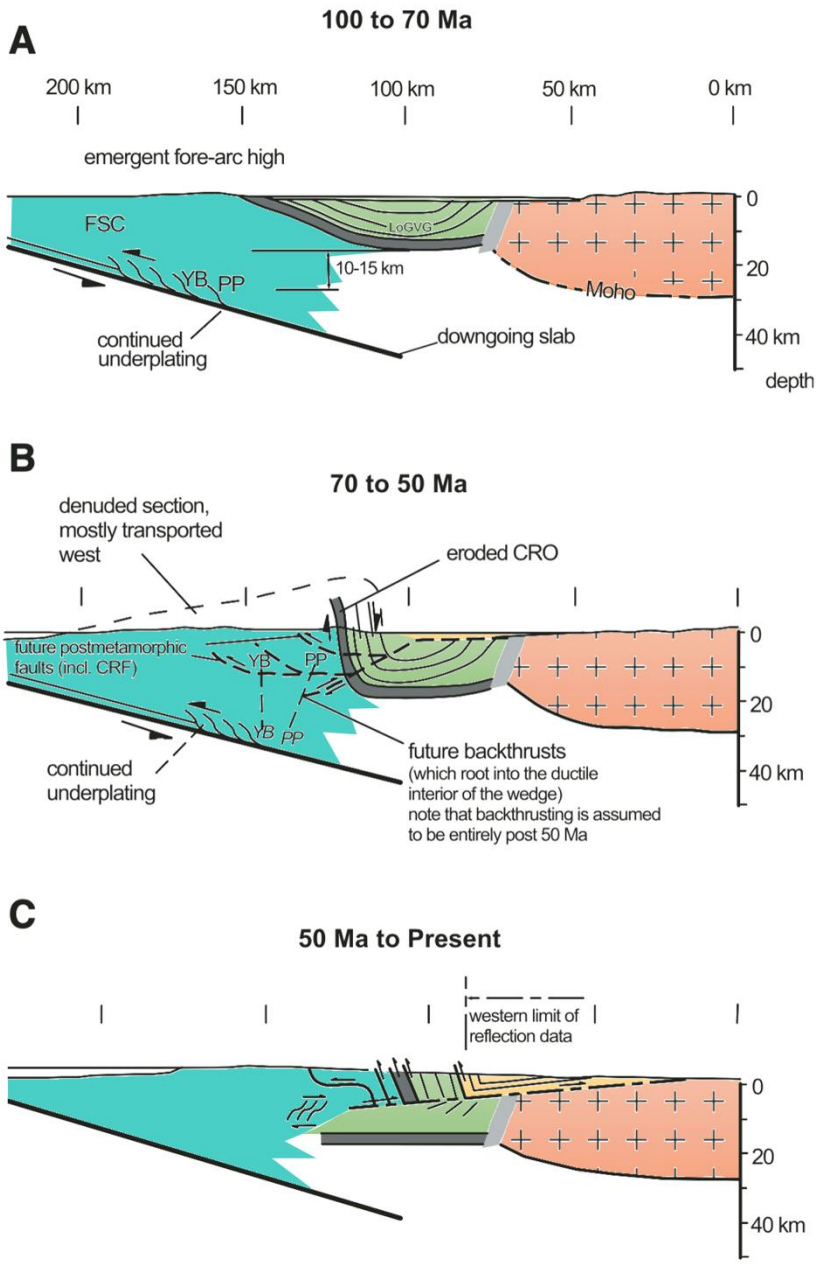


Figure 13. *Evolution of the Franciscan margin according Ring (2008).*

High-pressure metamorphism in Eastern Belt; forearc high became emergent probably at ca. 84 Ma; based on age of 50–70 Ma for oceanic crust, water depth was ~5.5 km and wedge thickness of 27.5 km, consistent with Yolla Bolly meta grade.

Main exhumation; normal faults in western Great Valley basin effect differential uplift and exhumation; Franciscan subduction complex (FSC) detritus occurs in Great Valley basin and in Franciscan itself.

Post-Paleocene E-directed back-thrusting & progressive accretion of younger Franciscan terranes at same time. Deformation in forearc basin causing concentration of deformation at forearc basin-wedge interface.

Ring (2008) extends his analysis of uplift and exhumation to address the timing and nature of deformation in the adjacent Great Valley fore-arc basin which further constrains the timing and kinematics of the deformation.

Stop 1: Pebbly Sandstone (Conglomerate) at Four Corners Area

Our field trip begins at an outcrop of pebbly graywacke sandstone on the southeast corner of Angel Island, inland from Point Blunt and on the inland side of the main road near the former Nike Missile site.

This outcrop consists mainly of metamorphosed graywacke sandstone that contains scattered rounded clasts of other rock types. Due to the presence of the rounded clasts, it can also be classified as a conglomerate. Look closely and you can find pebbles of chert, sandstone, basalt, and blueschists, all suspended in a sandstone matrix. All these clast lithologies are found widespread in northern California as part of the Franciscan subduction complex. The presence of blueschist minerals in this sandstone indicates that this rock experienced high pressure but relatively low temperature metamorphism along with most of the rocks on this island as a result of subduction and underplating.

Thick graywacke sandstone layers are a major component of the Franciscan in northern California and are typically interpreted as turbidites deposited from large turbidity flows. The scattered pebbles and unbedded character of this outcrop suggests that it represents a more viscous large submarine gravity flow called a debris flow, perhaps generated by the collapse of a sandy delta front. The large flows originated near the paleo shoreline, flowed downslope into the trench axis, and then were incorporated into the accretionary wedge by subduction.



***Stop 1. Photo 1**. Outcrop of pebbly sandstone at Four Corners area. Tom MacKinnon for scale.*



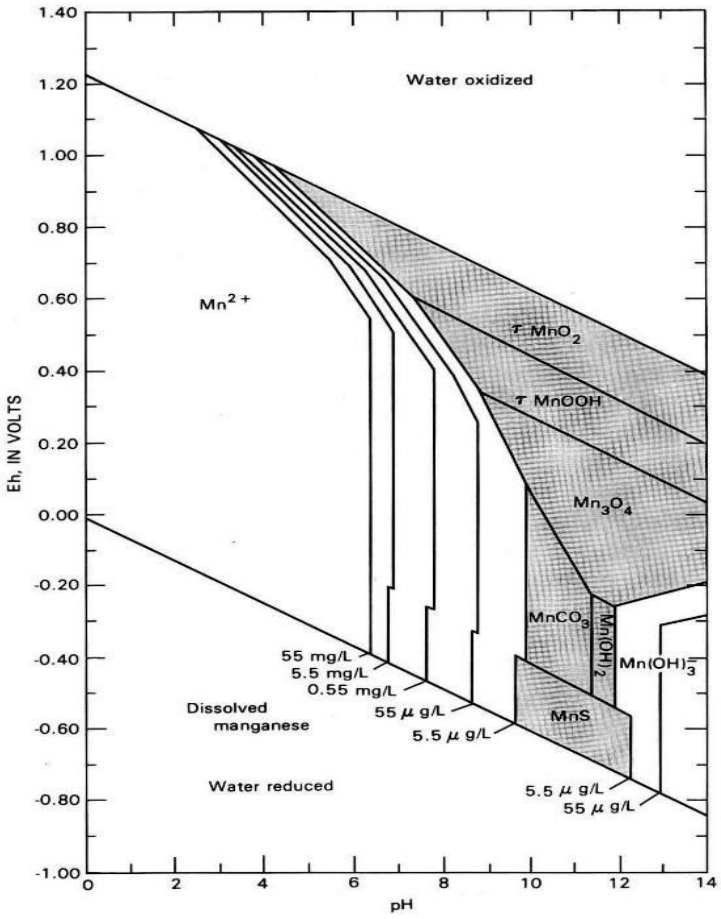
Stop 1. Photo 2*: Detail photo of pebbly graywacke sandstone. Pencil for scale. This sandstone is metamorphosed to blueschist grade, as are the imbedded pebbles.*



Stop 1. Photo 3: *The brown coating on the cobble imprints to the left of the hand is probably manganese minerals leached from the graywacke and deposited around the cobble by groundwater.*

Manganese minerals are abundant in Franciscan Complex chert sandstones, graywacke, and metagraywacke. We will see more manganese in the chert outcrop at Stop 7. Coast Range manganese (Mn) mineral deposits frequently occur in the Franciscan and, except for a few rare cases, are interbedded with red or green radiolarian chert according to Taliaferro and Hudson (1943). Manganese geology and geochemistry extracted and updated from Motzer and Petrofsky (2018).

Generally, unweathered graywacke is dark gray and unweathered sandstones (arenites) have a buff or tan hue. However, as manganese is leached from and subsequently deposited on fractures, joints, and fault surfaces, the rocks acquire a chocolate-brown hue. Examples can be seen at the Stop 1 outcrop and at other outcrops we will see later during this field trip..



Stop 1. Figure 1. *Eh-pH stability diagram for manganese (Mn) at standard atmospheric temperature and pressure (Hem, 1989). See text for discussion.*
The Eh-pH (redox) diagram in Figure 1 demonstrates how different soluble and insoluble manganese (mineral) species form when rainwater percolates downward in fractured rock to eventually become groundwater; and when subsequent weathering (oxidation) occurs. Solid Mn(IV) (in the gray shaded areas) and dissolved Mn(II) species occur over a wide pH range. For example, at a pH of ~7.5, Mn^{2+} soluble concentrations are ~0.55 milligrams per liter or mg/L [550 micrograms per liter (µg/L), or (ppb)].

Percolating precipitation (groundwater) is generally slightly acidic and acts as a relatively good solvent. However, as pH increases above 8 and 9 (i.e., becomes more alkaline, probably from dissolving of calcium carbonate cement), manganese solubility drops to 55 ppb and 5.5 ppb, respectively and as oxidation (weathering) increases, manganese oxides precipitate, occurring as insoluble manganese minerals such as pyrolusite (MnO_2), birnessite (δMnO_2), and hausmannite (Mn_3O_4).

Stop 2: Blueschist Graywacke

Directions: From Stop 1, walk west along the road approximately 500 meters (0.3 miles). The road is downhill for the first half of this distance then flat for the remainder.



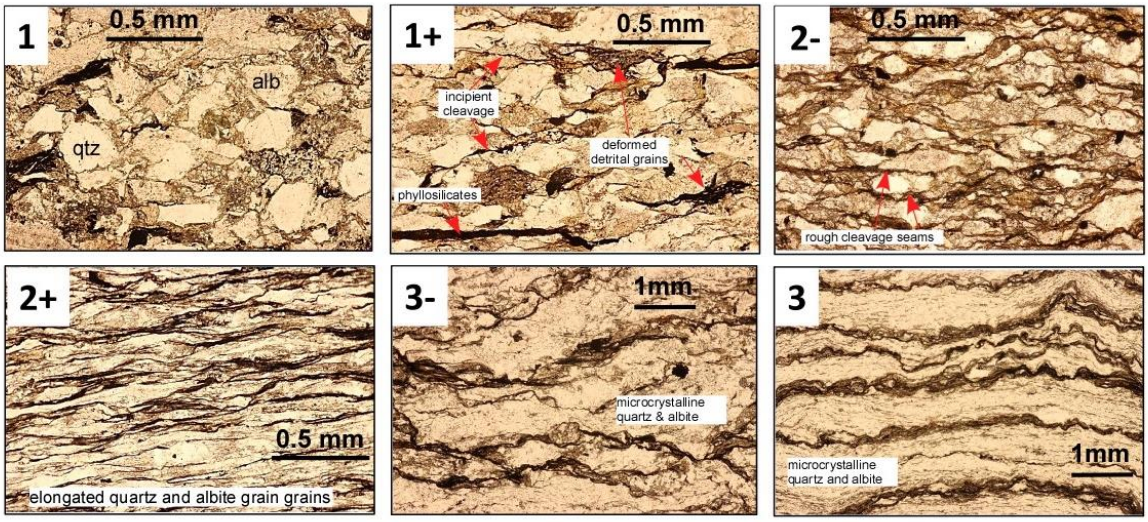
This stop gives us a view of a large outcrop of metamorphosed graywacke sandstone. The outcrop is a large exposure of the sandstone that forms a large part of Angel Island but is typically poorly exposed and gray color in outcrops. We will see numerous small examples along the road later in this trip.



Stop 2. Photo 1: *Large outcrop of textural grade 2 graywacke sandstone metamoprphosed to blueschist facies.*



***Stop 2. Photo 2**: Representative sample of metamorphosed sandstone at Stop 2.*



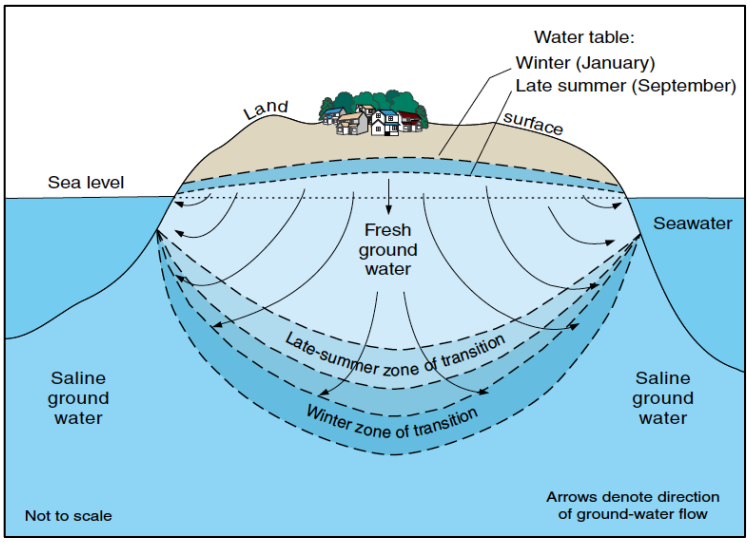
***Stop 2. Figure 1**: Classification system for sandstone textural grade* for *graywacke and graywacke precursors. **1** well-developed clastic texture. **1+** well-developed clastic texture with slight flattening of some grains and some disconnected dark-colored, matrix seams oriented roughly parallel to bedding. **2**- dark-colored matrix seams abundant and connected in an anastomosing web roughly parallel to bedding; flattening of clastic grains is apparent but clastic texture still clearly recognizable. **2+** strong foliation accentuated by finely spaced laminations of matrix alternating with partially recrystallized quartz/albite; some relic clastic grains still recognizable in thin section or in hand sample; some samples are largely recrystallized with some dominated by elongate quartz and albite grains. **3-** quartz and albite grains nearly completely recrystallized; well-developed segregated layers are notably thicker and a few corroded relic clastic grains usually present. **3** nearly complete segregation of fully recrystallized quartz/albite layers, typically 1 to 3 mm thick, separated by continuous to discontinuous bands of dark-coloured matrix.*

Stop 2 B: Water Supply and Hydrology of Angel Island

Background - Angel Island is a 770-acre island in San Francisco Bay. The highest point on the island is Mount Livermore at 781 feet. There are no surface water features on the island other than seasonal springs. Average annual precipitation is about 20 inches (Marin County, 2005).



Stop 2B Photo 1*. Drinking fountain*



Stop 2 B. Figure 1. *Generalized groundwater flow pattern of a homogeneous island aquifer (United State Geological Survey, 2000). Movement of the zone of transition and water table shown for winter and late summer. The Angel Island groundwater flow pattern is more complicated due to the bedrock fracture flow paths. However, the overall concept shown on Figure 1 is applicable to Angel Island.*

Water Supply - The water supply for the island is provided by four active wells and one standby well. The water system is operated by a licensed State Park Water and Wastewater Supervisor who oversees the operation, maintenance, and monitoring of the system. The water system serves the park visitors, concessions, park workers, and park residents. The wells range from 259 to 304 feet in depth. The groundwater quality is good based on historic sampling. No water treatment is required, but the water is chlorinated to provide additional protection. After the water is chlorinated, it is pumped into storage tanks on the island and then flows by gravity in a distribution pipeline system to the park users. The two large 500,000 gallon water storage tanks on the island were constructed by the WPA around 1940 (State Park Staff).

Water Quality - Even though the wells are drilled into an island surrounded by the brackish to saline water of San Francisco Bay, the chloride levels in the well water do not show saltwater intrusion. For example, all wells have chloride levels below the 100 milligrams per liter (mg/L) benchmark used by the California Department of Water Resources as a saltwater intrusion screening level and below the secondary maximum contaminant level (SMCL) for chloride in drinking water of 250 mg/L. San Francisco Bay water, by comparison, has chloride levels that vary up to 30,000 ppm. Figure 2B-1 is a simplified diagram of an island that shows the relationship of fresh groundwater to saline ocean waters. Angel Island groundwater occurs in

bedrock fractures which typically have lower pumping rates than sand and gravel aquifers. These lower pumping rates and more torturous flow paths likely aid in preventing saltwater intrusion.

Water Supply History - Historically, fresh water on the island was supplied from natural springs. During the Spanish and Mexican periods, these springs were a main attraction to passing ships in need of fresh water. Later, the US military drilled wells and brought fresh water to the island via ships. Because the supply of water is limited on the island, the Army pumped bay water for fire abatement into tanks around the island (Angel Island Conservancy, 2024).

Below are records from a 1966 Angel Island planning and history report commissioned by California State Parks (Marshall, McDonald, and Associates, 1966).

- 1875 - Post surgeon reported the water supply to be unsatisfactory.
- 1883 - Post Quartermaster reported water supply from eight springs. Mentioned O'Donnell's Canyon (east side) and Wilson's Canyon (south side).
- 1886 - More than $3,500.00 was reported spent in repairs to Camp Reynolds water system.
- 1886 - Permission was granted to install a windmill to improve the water supply. An undated manuscript map in the National Archives from between 1879 and1889 showed the site of windmill and tanks at Point Knox.
- 1912. Complaints appeared in San Francisco newspapers that the Quarantine Station was inadequate in view of the increased needs expected as a result of the Panama Canal completion. *The Panama Canal officially opened on August 15, 1914. Interestingly, the oldest documented water well was drilled in 1915 and is still in good service today (CA Department of Water Resources well log database).*
- 1921 - Difficulties of well drilling at Immigration Station were reported: slow and, to date, no satisfactory flow of water.
- 1927 - The water shortage became more acute. Exploration for new or better sources was conducted. Proposals for deepening of existing wells and increased storage were made.
- 1928 - A report containing data on every possible source of water on the Island was submitted to the Area Quartermaster Corps. It recommended an additional 250,000 gallon storage tank, continued exploration and drilling of wells in more promising locations. The daily average consumption of water was 150,000 gallons with storage capacity of 500, 000. All the water for military use was brought by boats. Both the Quarantine and Immigration Stations were considered to have enough supply from their two good wells. The transported water came from the Presidio.
- 1929 - Quartermaster 9th Corps Area rejected the Water Report of 1928, noting that the cost of proposed improvements at $50,000, and thus condemned the Island post to permanent dependence on transported water at a total cost of much more than $50,000.

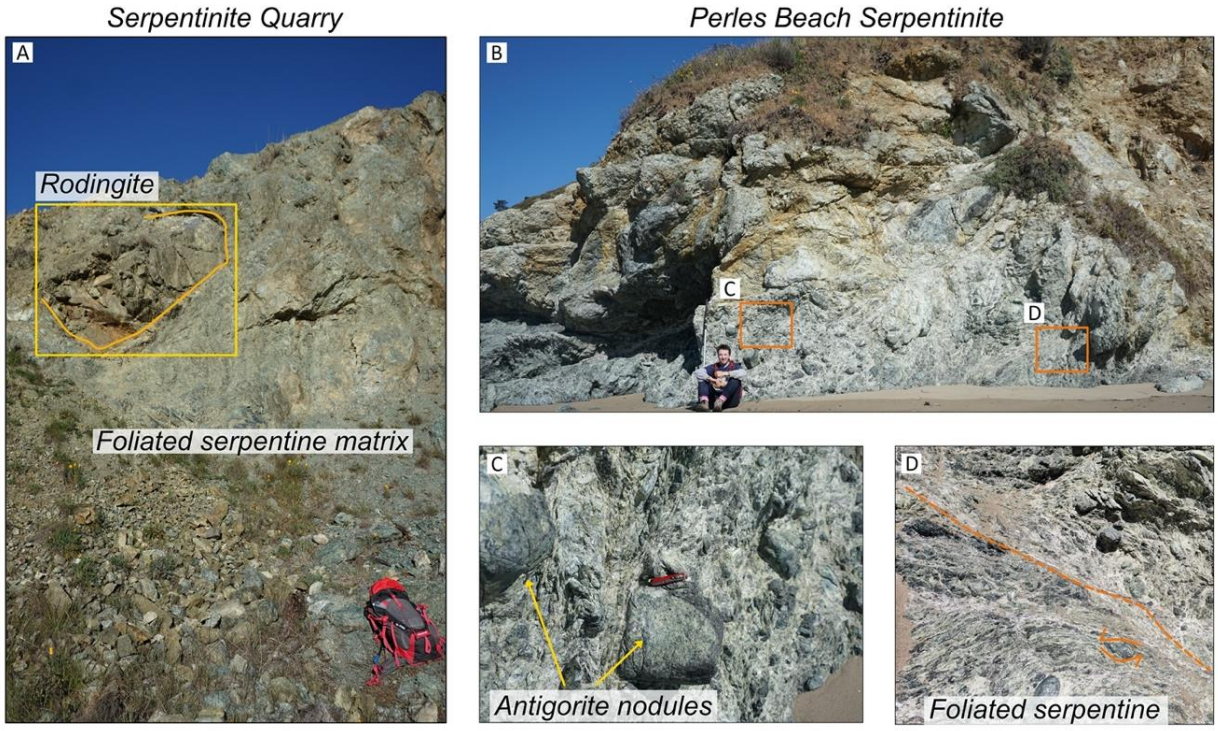
Wastewater Facilities - The Park's existing wastewater treatment facilities consist of a collection system, nine septic tanks, seven lift stations, a collection system of gravity-flow and force main sewer lines, and a secondary wastewater treatment plant (WWTP) to treat the pretreated effluent from the septic tanks. The WWTP consists of a flow equalization tank, a rotating biological contactor, a secondary clarifier, sludge removal facilities, and chlorination/dechlorination facilities. The effluent from the WWTP is pumped by force main to a subsurface soil disposal system (i.e., leach field) to dispose of all the effluent from the WWTP (Regional Water Quality Control Board, 2004).

Stop 3: Serpentinite Quarry

Directions: From Stop 2, proceed west along the road approximately 1050 meters (0.65 miles). The large outcrop is inland and uphill from the road, and easily visible from the road.



***Stop 3**: Map view of the perimeter road between Stop 2 and Stop 3.*



***Stop 3. Photo 1a-d (from Das, 2024):** Outcrops of foliated and nodular serpentinite at the Serpentinite Quarry and along Perles Beach. A: Large rodingite nodule embedded within a foliated serpentinite matrix in the Serpentinite Quarry. B, C, D: Outcrop of foliated serpentinite at Perles Beach that hosts antigorite nodules within it. The nodules are more resistant to weathering and stick out of the outcrop.*

The abandoned quarry along the southern Perimeter Road provides a very large exposure of serpentinite, California's state rock. Serpentinite is composed of serpentine, a mineral formed by hydration of ultramafic rocks (peridotite and others) from deep in the ocean crust and upper mantle. Serpentinite occurs in various shades of green and gray and has a shiny or waxy surface texture similar to snakeskin, hence the name derived from serpent. Various degrees of hydration create a variety of rock colors and textures in this quarry, which is part of the largest serpentinite body on Angel Island. This serpentinite body represents a fragment of the oceanic plate that was detached and incorporated into the accretionary prism during subduction, eventually becoming part of the Angel Island terrane.

The serpentinite in the quarry is pale green, feels very slippery, and is intensely foliated. This foliated serpentinite contains ovoid masses of very dense serpentine, usually darker green in color. In places there are also ovoid masses of other rocks within the serpentinite, including gabbro, sandstone, and metamorphic rocks. Some of these metamorphic rocks were formed by alteration of basalt or diabase inclusions within the serpentinite. (Konigsmark).



***Stop 3. Photo 2**: Outcrop photo of serpentinite showing a typical variety of colors and textures.*

Near the abandoned quarry is a large rock crusher built by the U.S. Army. The crushed serpentinite was used for road building on Angel Island and for construction of a dam to the east of the quarry. If you look for gaps in the asphalt pavement along the Perimeter Road, you can see the green serpentinite rocks that were used as the road base in many places.

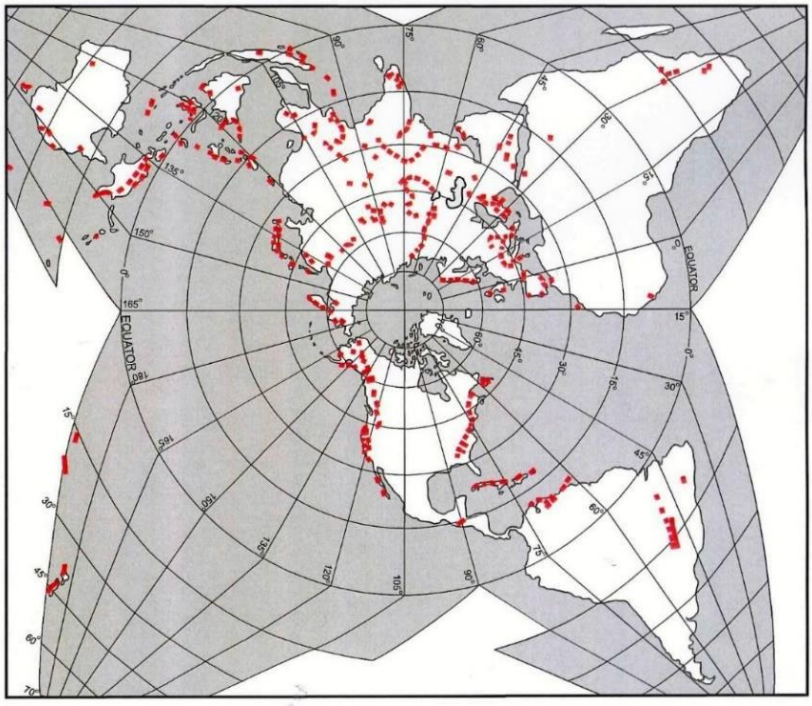
World-wide, serpentinites are volumetrically minor when compared to other rock-types. However, they are very common in ancient orogenic belts, particularly in ancient subduction and suture zones and in modern (current) subduction zones. When serpentinites occur with other rocks such as felsic and mafic volcanic basalt, ultramafics (UMs, e.g., harzburgite or peridotite) and minor chert, the suite is collectively named an ophiolite. These rocks occur on all continents, including Antarctica. Serpentinite and serpentinized peridotite comprise about 3 percent of Earth's surface rocks (Guillot and Hattori, 2013)

<u>Serpentinite Mineralogy and Geochemistry</u>

Serpentinite is a metamorphic rock composed of one or more (up to 20) serpentine group rock-forming minerals that are predominantly hydrous magnesium iron phyllosilicates [e.g., (Mg, Fe)3Si2O5(OH)4)], containing trace to minor amounts of other elements including chromium (Cr), manganese (Mn), cobalt (Co) or nickel (Ni). Because of varying admixtures, some varieties are not always easy to characterize in hand specimen. Three important minerals, antigorite, chrysotile, and lizardite, are formed by the serpentinization, a hydration and metamorphic transformation of mafic and UM rocks. There is some recent evidence suggesting that deep ocean microbial communities contribute or participate in the hydrogen generating reactions that convert UM to serpentinite in the following reaction for olivine (Templeton, 2011):

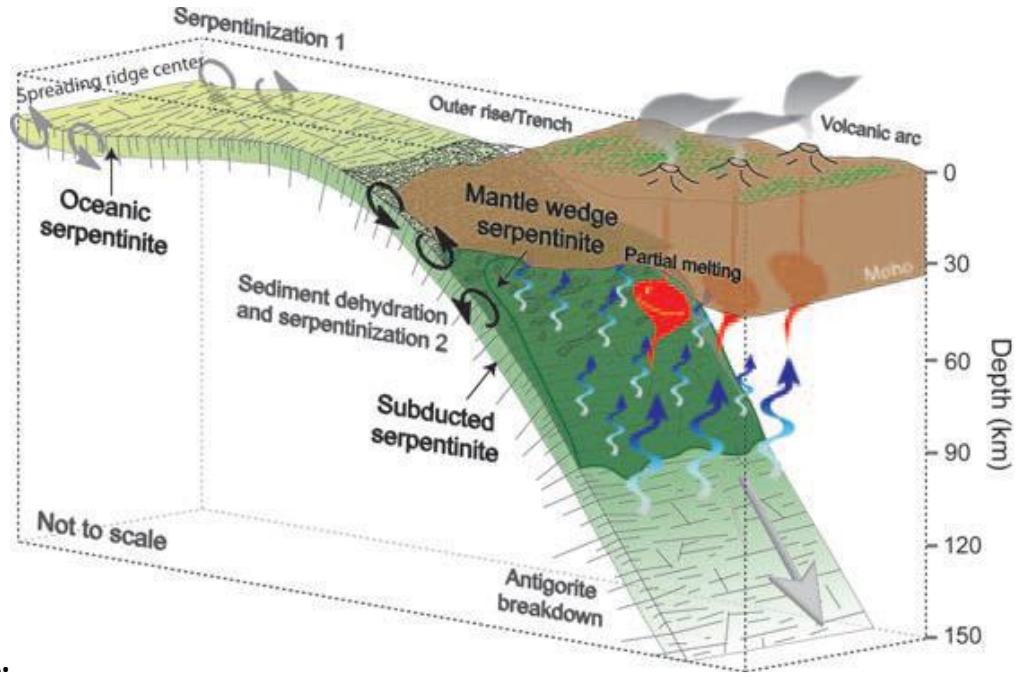
$Mg_{1.8}\ Fe_{0.2}\ SiO_4 + 1.37H_2O \rightarrow 0.5Mg_3\ Si_2O_5(OH)_4 + 0.3Mg(OH)_2 + 0.067Fe_3O_4 + 0.067H_2$

(olivine) (water) (serpentine) (brucite) (magnetite) (hydrogen)

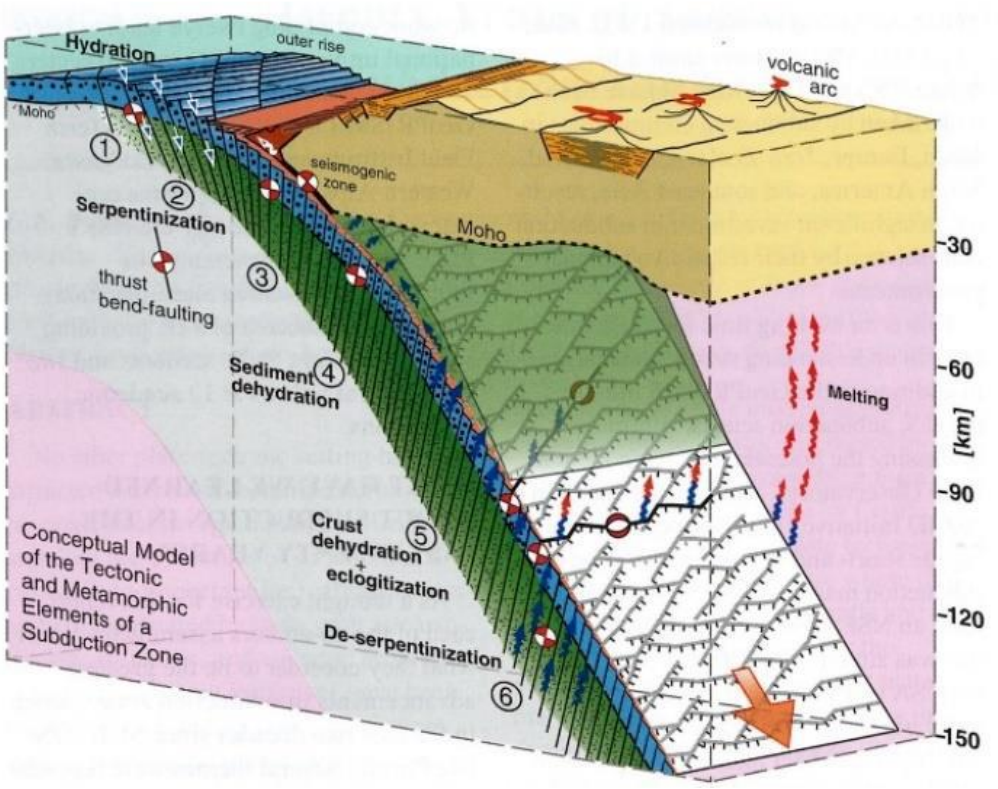


Serpentinization is important at sea floor and tectonic plate boundaries, particularly at subduction zones (Figure 2) (Evans, et al., 2013; Guillot and Hattori, 2013, Bebout, et al., 2018) and as shown in Figure 3.1.

Stop 3. Figure 1: *North polar projection showing world-wide serpentinite and ophiolite distribution (red squares) (Modified from Oze, et al., 2007).*



A.



B.

Stop 3. Figure 2*: Conceptual subduction zone-related models showing oceanic slab serpentinization.* ***A****: oceanic and subducted-related serpentinization from Guillot and Hattori (2013).* ***B****: fast subduction model from spreading center showing metamorphic evolution (Bebout, et al., 2018).*

Stop 4. Perles Beach

Directions: Proceed from Stop 3 about 800 meters (0.5 miles) to a sign indicating the trail downhill to Perles Beach. Carefully walk down the moderately steep trail to the beach. Hiking poles are highly recommended. We will examine several features along the length of this beach before returning up to the perimeter road using this trail. Perles Beach is a long shoreline exposure extending from serpentinite on the east end to metamafics and pillow basalts on the western end. The beach is reached by a moderately steep path with some metal stairs near the bottom. The vertical distance from the perimeter road down to the beach is approximately 50 m (160 feet). Everyone should move slowly and carefully down the path to the beach. Hiking poles are recommended for better stability on the steeper parts of the path.



Stop 4: Map view of perimeter road from Stop 3 (serpentinite quarry) to Perles Beach.



Stop 4. Photo 1: *Start of the path down to Perles Beach. This path entrance is minimally signed but is just before reaching a picnic and viewing area along the Perimeter Road. View of Alcatraz Island and downtown San Francisco in the distance.*

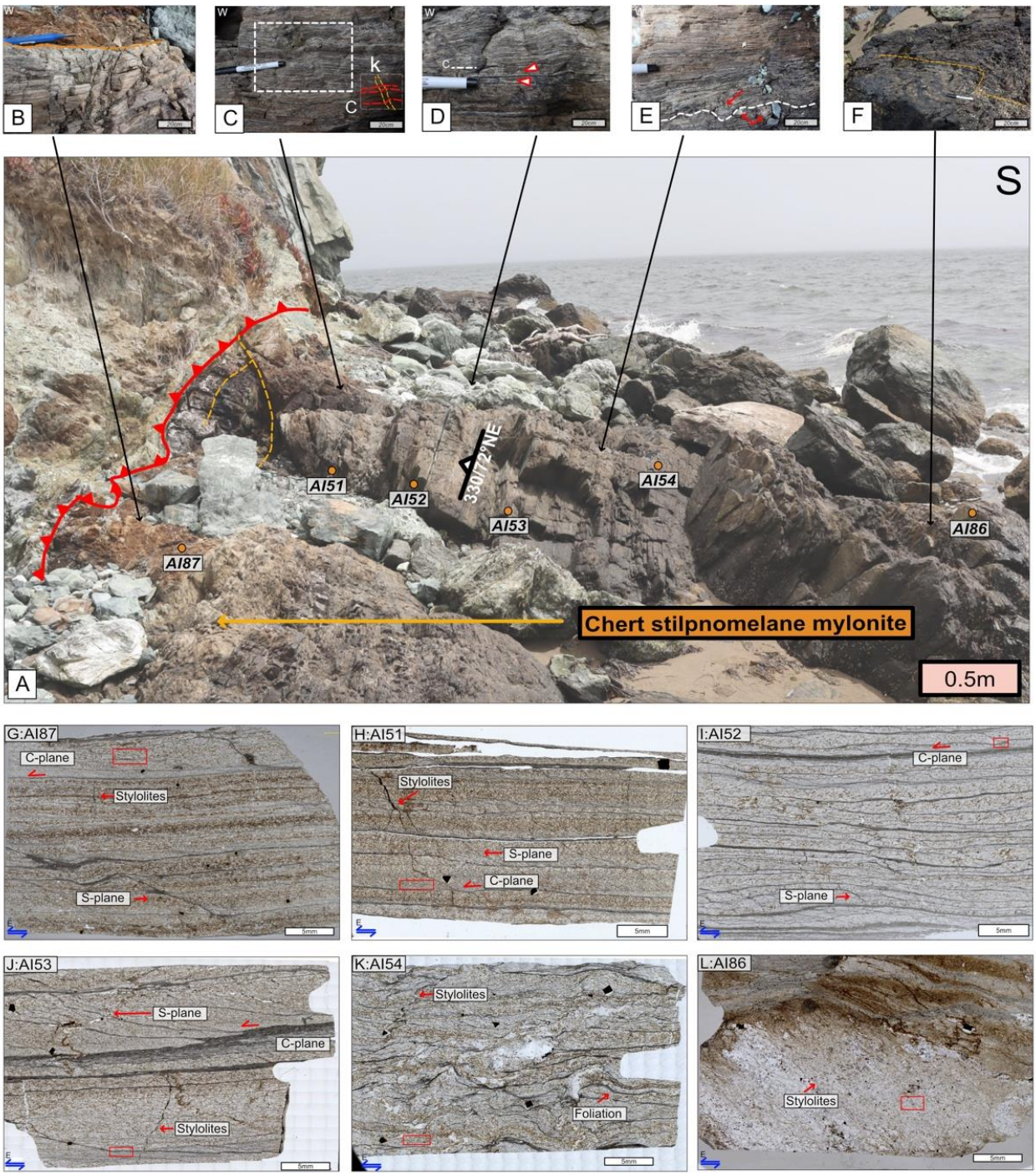
Perles Beach extends across the transition between a thick unit of serpentinite that cuts northwest across Angel Island and the pillow basalts and schistose sandstone that form the west end of Angel Island (Fig. 9). The broad but poorly exposed contact zone contains a variety of schists particularly near the east end of the beach. Pillow basalts and associated metamorphosed mafic rocks form the western part of Angel Island at the west end of the beach.

East End of Perles Beach: Meta-mylonite, ultra-fine crystalline fault zone

Outcrops at the east end of Perles Beach show a variety of schists and associated metamorphic rocks, particularly serpentinite. The geologic map (Figure 9) shows that these exposures are extensions of the large belt of serpentinite that extends diagonally across the southwest corner of Angel Island. Shoreline weathering has created some different views of the serpentinite that we saw in the quarry at Stop 3.

Near the eastern end of the beach, the serpentinite includes some large blocks of meta-morphosed sandstone and a few boulders of metamorphosed Franciscan chert. There are also layers of blueschist within the serpentinite complex, with the dark blue color from minerals such as lawsonite and glaucophane the form in unusual settings of high pressure but relatively low temperature. Laboratory studies show that these blue minerals form at pressures equivalent to rock burial depths of 12 to 30 miles and at temperatures of 100 to 300 degrees C. Normal temperatures at these depths are well over 300 degrees C. These conditions indicate burial deep in a subduction complex but then fairly quickly being brought back to the surface before the blueschist minerals are changed by higher temperatures normal to these depths.

East of the sandy beach, a rocky area exposes highly deformed rock representing a shear zone that formed as part of the megathrust separating subducting from accreted material. Das's (2024) description and analysis of this area is shown in photo 4.2.

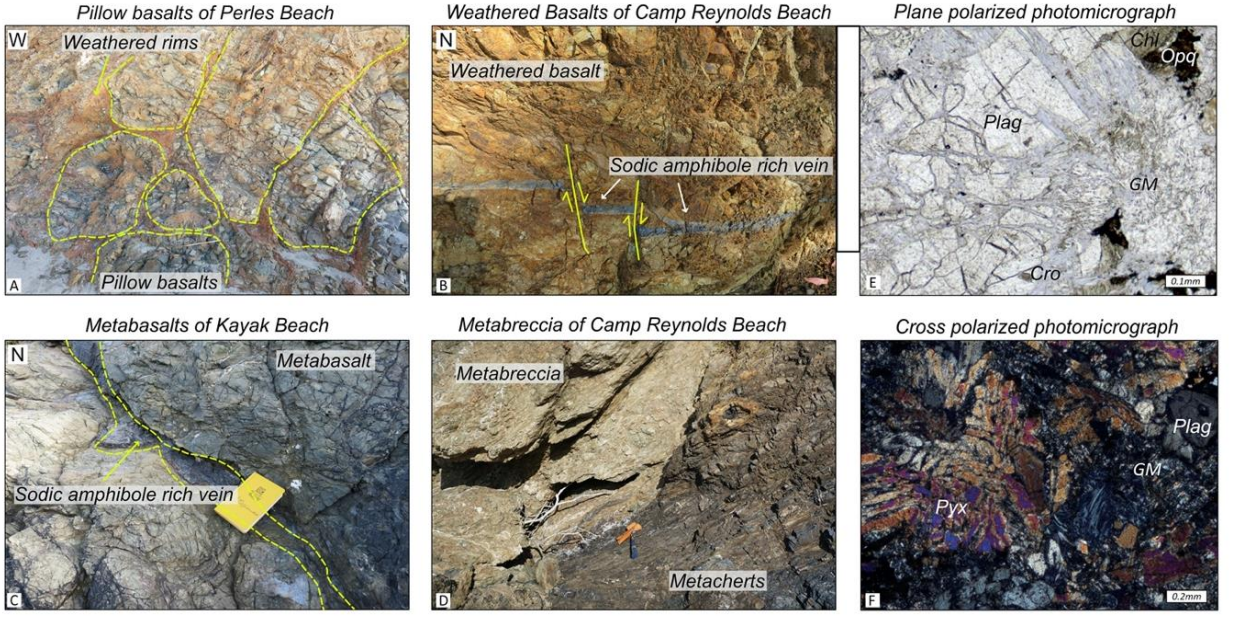


***Stop 4. Photo 2 from Das (2024)**: Outcrop photos and photomicrographs of Perles Beach thrust metachert mylonite. **(A)** Sampled transect of the metachert mylonite across a gradient in foliation spacing towards the fault core boundary. The locations of the samples are marked on the outcrop that shows an average foliation dipping 72°NE. Red thrust line indicates contact between mylonite and crosscutting chlorite schist zone. **(B)** Contact zone between the metachert mylonite with the velvety-brown alteration zone overprinting the structurally highest mylonite (orange dashed line). **(C)** Kinks within the mylonitic foliation with the relations between the*

foliation (c) and kink fold axial surface (k) shown as an inset within the white dashed box. ***(D)*** *Mylonitic foliation with S-fabric (red arrowheads) intersecting with C-planes.* ***(E)*** *Wavy foliation with rotated chert boudins (red arrows) transitioning to planar foliation upsection (north).* ***(F)*** *Bedded metachert at the water line, farthest from the fault core marked by the development of bedding/foliation composite fabric (orange dashed lines) and axial planar cleavage. Asymmetric fold indicates apparent east vergence.* ***(G-L)*** *Photomicrographs (ppl) of metachert mylonite with their corresponding location within the outcrop. The mylonites show increasing planarity of the foliation surface with progressive development of shear fabric and stylolites. All the samples contain the same phases of quartz, riebeckite, stilpnomelane and pyrite in varying proportions. All samples show a top-to-the-southeast shear sense.* ***(G-K)****: Strong wavy mylonitic foliation formed by flattening, shear, and transposition of bedded metachert.* ***(L)*** *Contact between riebeckite schist (top) and metachert (bottom).*

West End of Perles Beach: Meta pillow basalts and associated blueschist mineral veins

The middle part of Perles Beach has very sparse outcrops due to vegetation and soil overburden. The western end of Perles Beach has extensive outcrops of pillow basalts that form most of the western end of Angel Island. Individual pillows are about a foot thick and two to three feet long, and occasionally are separated by thin layers of chert or metamorphosed



Stop 4. Photo 3 from Das (2024)*: Field and microscopic characteristics of metabasalts on Angel Island.* ***A****. Pillow basalts on the western end of Perles Beach with weathered rims.* ***B****. Amphibole vein cross-cutting across weathered basalts.* ***C****. Metabasalts with amphibole vein along the contact.* ***D****. Metabreccia consisting of clasts of metabasalts juxtaposed against blue-brown bedded chert.* ***E and F****. Photomicrographs highlighting the plagioclase, pyroxene embedded within a crossite and chlorite matrix. Abbrev: Plag (plagioclase), Pyx (pyroxene), Chl (chlorite), GM (groundmass), Opq (opaque), Cro (crossite).*

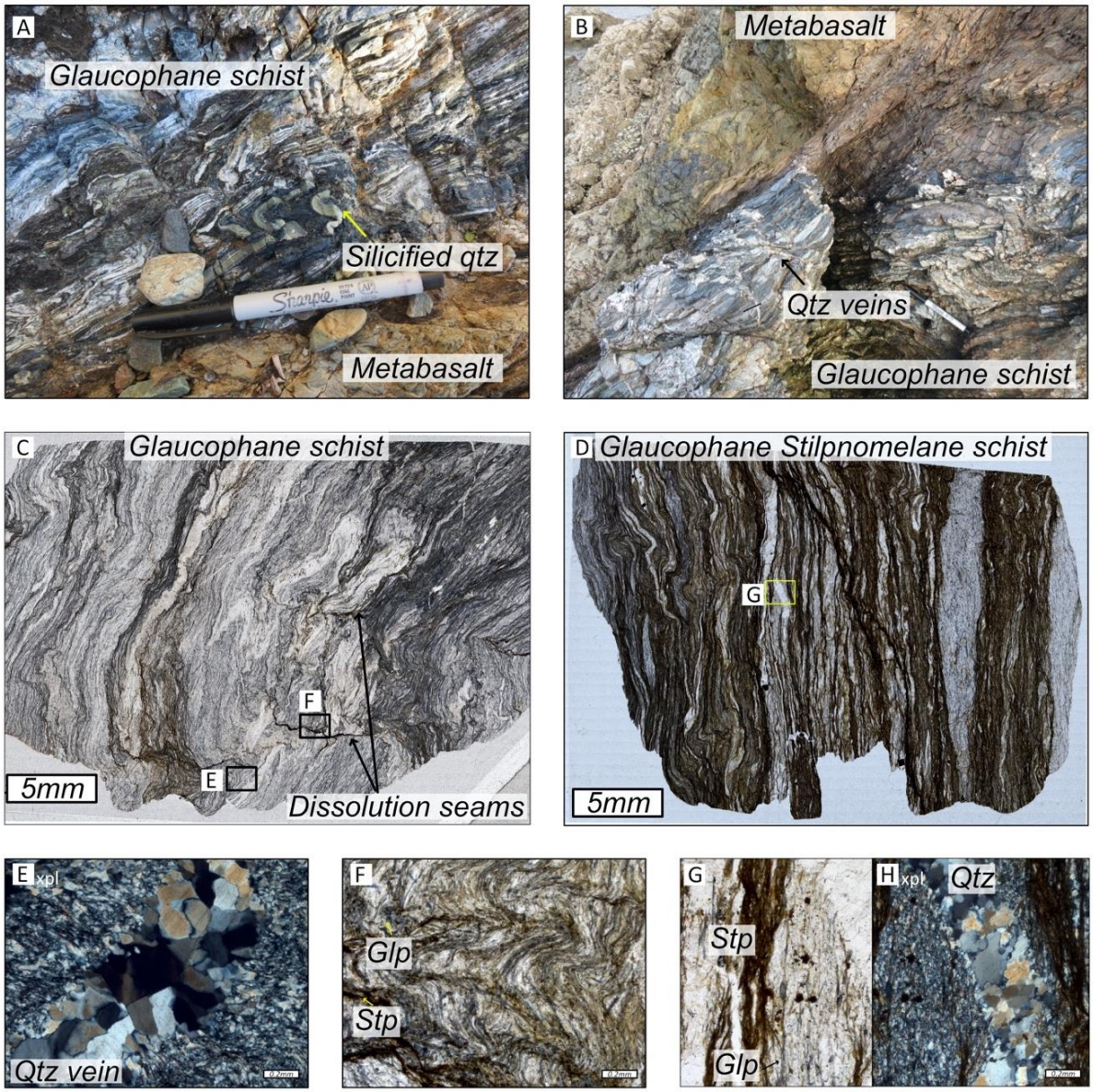
The clearest basalt pillows have glassy rims that represent rapid quenching of the molten lava against cold seawater on the deep sea floor (photo 4.5). Sets of basalt pillows form layers a few feet thick that dip steeply to the northwest. The lack of vesicles in the basalt pillows indicates they were extruded in very deep water which kept dissolved volatiles from expanding into bubbles as the magma rapidly cooled on the sea floor.



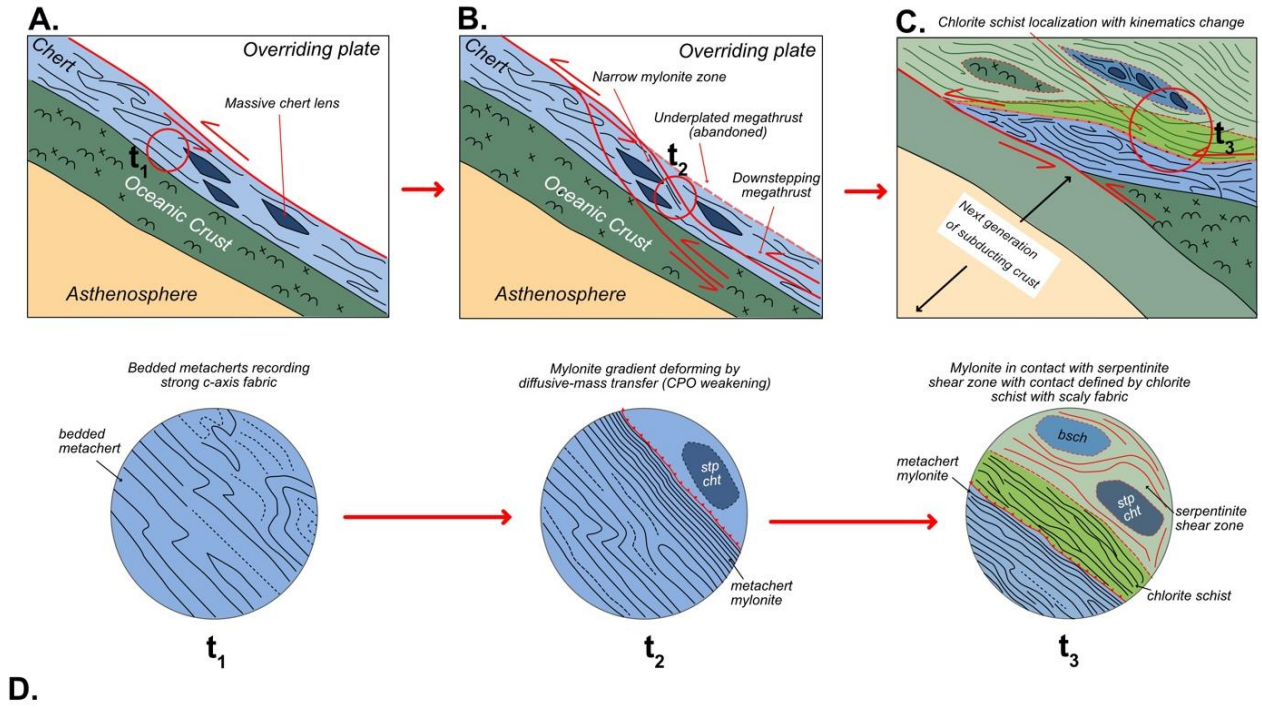
Stop 4. Photo 5*: Detail of chilled margin of a pillow basalt at Perles Beach.*

Although the pillow basalts appear brown on the weathered surfaces, laboratory analyses show that these basalts have been metamorphosed to blueschist facies like most of the rest of the rocks that make up Angel Island. Original pyroxene and feldspar crystals have been altered to chlorite, lawsonite, glaucophane and other metamorphic minerals (photo 4.3), but the blue metamorphic minerals are not abundant enough to give the metabasalts a distinct blue color. Instead, the outcrops are generally brown, probably due to precipitation of manganese minerals, as described in the Stop 1 section.

Juxtaposed to the minimally-deformed basalt pillows are highly deformed glaucophane schists. These are illustrated and described by Das (2024) (Photo 4.6).



Stop 4. Photo 6, from Das (2024)*: Field characteristics and photomicrographs of glaucophane schists along the contacts with metabasalts.* ***A and B****: Outcrops of glaucophane schists with silicified quartz and quartz vein cross-cutting the foliation.* ***C and D****. Photomicrographs of glaucophane and glaucophane-stilpnomelane schists highlighting the compositional layering between blue glaucophane rich domains and brown stilpnomelane rich domains with dissolution seams cutting across the layering.* ***E and F*** *are insets from* ***C. E****. Crossed polarized image of quartz vein showing undulose extinction and suture grain boundaries.* ***F****. Folded stilpnomelane and glaucophane needles.* ***G and H*** *are insets from* ***D*** *with plane and crossed polarized images of quartz vein cutting across a stilpnomelane foliation surface. Abbrev: Qtz (quartz), Glp (glaucophane), Stp (stilpnomelane).*



Stop 4. Figure 1, from Das (2024)*: Schematic cross-section of subduction zone with relation between overriding plate, chert section, oceanic crust and asthenosphere. The megathrust is shown in red.* ***Red circles*** *indicate the stage of fabric development in* ***D****.*

(A) and t1*: Folding and flattening by dislocation creep as the chert section subducts under the overriding plate, developing strong c-axis fabric at blueschist facies.*

(B) and t2*: As the megathrust stepped down into the oceanic crust, the Perles Beach thrust mylonite was formed including the massive chert lenses. The mylonite deforms by diffusive mass-transfer mechanism that reduces c-axis fabric.*

(C) *Due to imbrication and underplating, Perles Beach mylonite came into thrust contact with serpentinite forming a contact reaction zone of chlorite schist which includes blocks of mylonite and massive chert.*

(D) and t3*: Inclusion of metachert and metabasalt slices into serpentinite shear zone. Metachert juxtaposed against a serpentinite matrix marked by the development of sodic amphibole-chlorite schist along the contact.*

Abbrev: stp cht (stilpnomelane chert), cht(chert), bsch (blueschist).

Stop 5. Kayak Beach

Directions: Climb back up the trail from Perles Beach to the main road and proceed west and then north to a large red building. The trail down to Kayak Beach begins past the restrooms.



The trail down to Kayak Beach leads through undergrowth beneath trees. Be careful of your footing and beware of poison oak near the trail. The trail is a moderate downgrade at first but becomes steeper near the beach. Take your time and be cautious!



Stop 5. Photo 1: Serpentinite boulders near the south end of Kayak Beach, looking northward.

On Kayak Beach series of graywacke sandstones and conglomerates are exposed between the serpentinite shear zone on the south and the Dead Hawk fault zone mapped by Das (2024) on the north. We begin our beach walk just east of the serpentinite shear zone and walk north towards but not to the Dead Hawk fault zone. As we walk, observe the variability of sandstone grain size and degree of deformation. For example, a large boulder of boulder conglomerate is exposed on the beach, having most likely rolled down the adjacent bluff (Photo 5.2). Clasts in it are little deformed. In contrast, towards the north end of the beach, conglomerates are more deformed with highly stretched shale clasts.

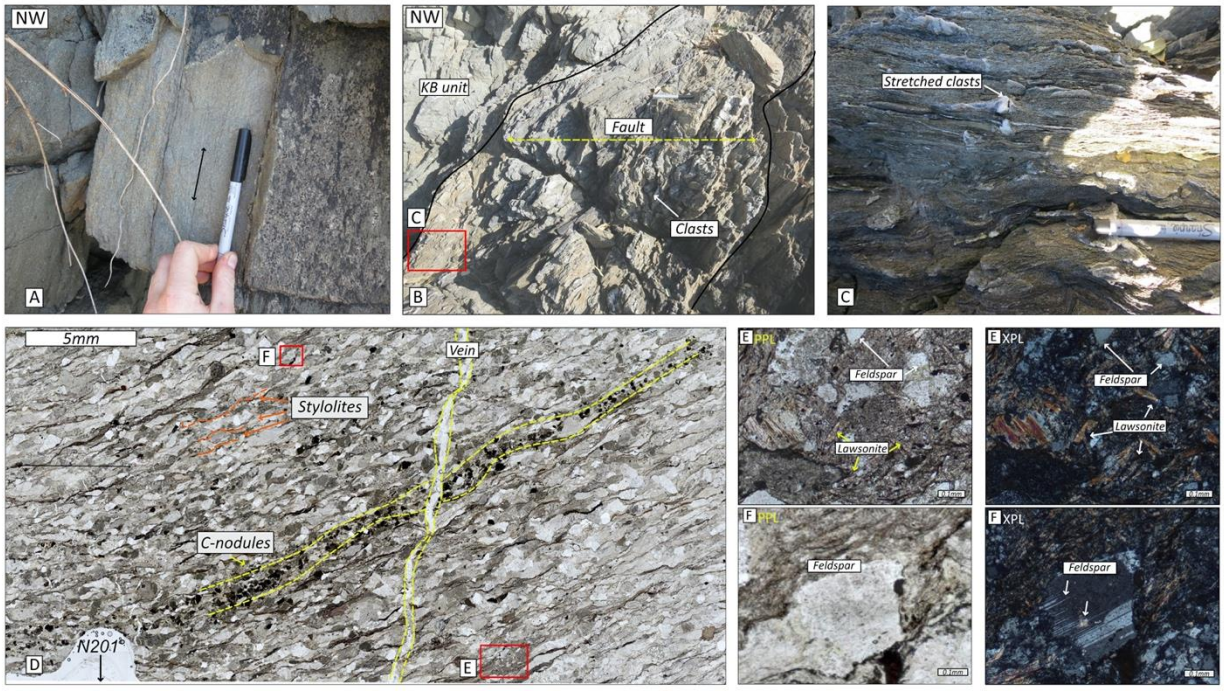
Das (2024) illustrates and describes deformation fabric and microstructures in photo 5.4.



***Stop 5. Photo 2**: Conglomerate or mélange block near the center of Kayak Beach*



***Stop 5. Photo 3**: Close-up of pebbly graywacke at north end of Kayak Beach*



Stop 5. Photo 4 (from Das 2024): Kayak Beach metagraywacke outcrop and microstructures.
A) Close-up of the grain shape fabric (parallel to black arrow) on the outcrop.
B) Fault zone (yellow dashed arrow) within the conglomerate horizon (bounded by black lines).
C) Stretched clasts within a shear zone.
D) Photomicrograph showing presence of through-going cross-cutting quartz veins (yellow dashed), stylolites (orange dashed) and carbonaceous nodules (C-nodules).
E) Growth of lawsonite laths in the matrix (yellow and white arrows) in plane and crossed polars with feldspars.
F) Feldspar showing deformation twin lamellae.
Das, M., 2024

Stop 6. Blueschist Graywacke near Point Ione

Directions: From Kayak Beach, hike back up the trail to the perimeter road and turn left to walk northwest on the paved road for about 15 minutes. Look for the outcrop shown in photo 6-1.



Stop 6: Map view of path from Kayak Beach to sandstone outcrops along the Perimeter Road.



Stop 6. Photo 1*. Fractured blueschist graywacke sandstone near Point Ione*

Much of Angel Island consists of schistose sandstone, including outcrops at the Four Corners area seen at Stops 1 and 2 (reference to geologic map, Figure 9). Numerous smaller outcrops occur along the western side of the island along the Perimeter Road, but vegetation partly covers many of these outcrops. This stop provides a brief view of the best example of these schistose sandstone outcrops on the west side of the island, and allows us to compare these rocks to the sandstones seen earlier in this field trip.

Although the sandstone in this outcrop appears darker than at Stops 1 and 2, fresh pieces that have fallen on the roadside show that the actual character is very similar to those outcrops. Pebbles are rare in this outcrop but do occur in some nearby outcrops.

The original graywacke sandstone has undergone moderate metamorphism due to high pressures after being subducted and deeply buried. With a hand lens you can see that the schistose character of this sandstone is due to thin layers of small flattened grains that cause the sandstone to separate into roughly tabular pieces. The flattening likely follows original bedding of the sandstone and is parallel to the rough bedding seen in parts of this outcrop. Thin layers of clay and silt between the sandstone layers in the original turbidite beds developed a more schistose fabric that helps to define some of the original bedding character.

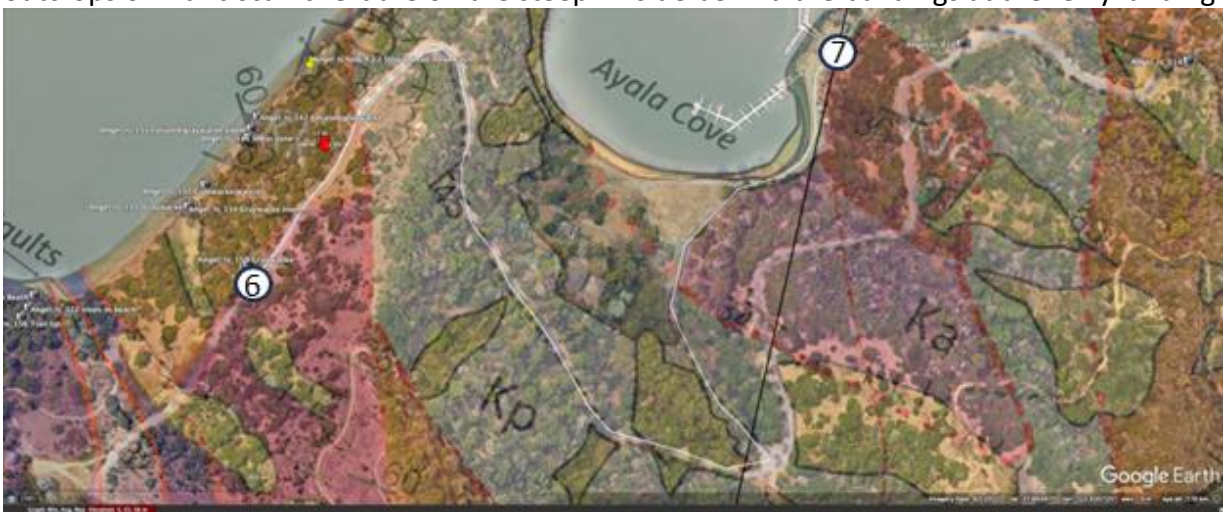


***Stop 6. Photo 2**: Possible relict bedding in schistose sandstone. Weeds for scale.*

Thin sections show that some sandstone grains have been replaced by metamorphic minerals such as lawsonite, showing that these rocks are of blueschist facies as are most of the rocks on Angel Island. Where present, pebbles show flattening along the same orientations as the schistose fabric, consistent with deformation under high pressures deep in the subduction complex.

Stop 7. Franciscan Red Chert near Ferry Dock

Directions: Follow the main road north and then northeast to reach the Ferry Dock. The outcrops of Franciscan chert are on the steep hillside behind the buildings at the ferry landing.



Stop 7: Map view of the trail from Stop 6 to Stop 7.



Stop 7. Photo 1: *Outcrop of red chert in the cliff just behind the ferry dock at Ayala Cove.*

Outcrops of Franciscan red chert can be seen in the cliffs behind the ferry dock. These distinctly layered and folded rocks form prominent dark red outcrops and rocky slopes in several parts of Angel Island. The chert was deposited on the deep ocean floor far from land, and gradually

brought toward North America by subduction. Silica skeletons of plankton called Radiolaria settled to the ocean floor along with clay particles to form a silica ooze that slowly accumulated as the ocean crust migrated from the mid-Pacific spreading center toward the continent. Over tens of millions of years, the siliceous ooze solidified into chert and shale. Subduction and underplating caused extensive deformation to the thin chert layers. The typical red color comes from small amounts of iron oxides deposited from iron-rich dust blown to the mid Pacific from distant Asia deserts. Larger outcrops of Franciscan chert occur on the north side of the Golden Gate Bridge.

Conclusion to the field trip

The field trip officially ends at the Angel Island ferry dock.

Acknowledgements:

The authors thank Dr. Meg Das and Dr. Christine Rowe for leading advance trips to Angel Island and sharing prepublications. We also thank members of the California State Park system for their help with the logistics of preparing for and conducting the field trip.

References

Agard, P., Plunder, A., Angiboust, S., Bonnet, G, Ruh, J., 2018, The subduction plate interface: rock record and mechanical coupling (from long to short timescales). Lithos, Elsevier, 2018, 320-321, pp.537-566.

Angel Island Conservancy, 2024. https://angelisland.org/

Apen, F.E., Wakabayashi, J., Day, H.W., Roeske, S.M., Souders, A.K., and Dumitru, T.A., 2021, Regional-scale correlations of accreted units in the Franciscan Complex, California, USA: A record of long-lived, episodic subduction accretion, in Wakabayashi, J., and Dilek, Y., eds., Plate Tectonics, Ophiolites, and Societal Significance of Geology: A Celebration of the Career of Eldridge Moores: Geological Society of America Special Paper 552, p. 233–255.

Bailey, E.H., Irwin, W.P., and Jones, D.L., l964, Franciscan and Related Rocks, and their Significance in the Geology of Western California: California Division of Mines and Geology, Bulletin, v. l83, l77p

Bebout, G.E., Scholl, D.W., Stern, R.J., Wallace, L.M., and Agard, P., 2018, *Twenty Years of Subduction Zone Science: Subduction Top to Bottom 2 (ST2B-2)*: GSA Today, v. 28, n.2, pp. 4-10.

Berkland, J.O., Raymond, L.A., Kramer, J.C., Moores, E.M., and O'Day, M., 1972, What is Franciscan?: American Association of Petroleum Geologists Bulletin, v. 56, p. 2295–2302.

Blake, M.C., Jr., ed., 1984, Franciscan Geology of Northern California: Pacific Section Society of Economic Paleontologists and Mineralogists Book 43.

Blake, M.C., Jr., Graymer, R.W., and Jones, D.L., 2000, Geologic Map and Map Database of Parts of Marin, San Francisco, Alameda, Contra Costa, and Sonoma Counties, California: US Geological Survey Miscellaneous Field Studies Map MF-2337, version 1.0, 1 sheet, and Pamphlet, 31p.

Curry, F.B., Cox, A., and Engebretson, D.C., 1984, Paleomagnetism of Franciscan rocks in the Marin Headlands, in Blake, M.C., Jr., ed., Franciscan Geology of Northern California: Los Angeles, California, Pacific Section, Society for Economic Paleontologists and Mineralogists (SEPM), Book 43, p. 89–88.

Das, M., 2024, *Subduction Sandwich: Investigating the Evolution and Deformation of a Subduction Plate Boundary Interface from the Overriding to the Downgoing Plate*: PhD Dissertation, Department of Earth and Planetary Sciences, McGill University, Montréal, Québec, 161 p.

Ernst, W.G., 2017, Geologic evolution of a Cretaceous tectonometamorphic unit in the Franciscan Complex, western California: International Geology Review, v. 59, p. 563–576.

Evans, B., Hattori, K., and Baronnet, A., 2013, *Serpentinite, What, Why, Where?*: Elements magazine, v. 9, n. 2, pp. 107-113.

Guillot, S. and Hattori, K., 2013, *Serpentinites: Essential Roles in Geodynamics, Arc Volcanism, Sustainable Development, and the Origin of Life*: Elements magazine, v. 9, n. 2, pp. 95–98.

Hem J.D., 1989 (third edition), *Study and Interpretation of the Chemical Characteristics of Natural Water:* U.S. Geol. Survey Water Supply Paper 2254, USGS, Alexandria, VA, 263 p.

Irwin, William P. (1990). "Geology and plate-tectonic development". In Robert E. Wallace (ed.). The San Andreas Fault System, California, U.S. Geological Survey Professional Paper 1515. pp. 61–82.

Kimura, G., Maruyama, S., Isozaki, Y., and Terabayashi, M., 1996, Well-preserved underplating structure of the Franciscan complex, Pacheco Pass, California: Geology, v. 24, p. 75–78.

Konigsmark, T., 1998 (third printing 2006), *Geologic Trips: San Francisco and The Bay Area*: GeoPress, Gualala, CA, 174 p. ISBN: 0-9661316-4-9.

Marin County, 2005. Hydrology and Water Quality of Marin County.

Marshall, McDonald, and Associates, 1966. Report and Recommendations on Angel Island, 1769 to 1966. Recommendations for the Historical Recreational Development of Angel Island.

Motzer, W.E. and Petrofsky, M., 2018, *Field Guide to the Unique Geology/Geochemistry of Ring Mountain Open Space Preserve (RMOSP), Marin County*: Northern California Geological Society (NCGS), 30 p.

Oze, C., Bird, D.K., and Fendorf, S., 2007, Genesis of Hexavalent Chromium from Natural Sources in Soil and Groundwater: Proceedings of the National Academy of Sciences (PNAS), v. 104, n. 16, pp. 6544–6549.

Peacock, S.M., 2020, Advances in the thermal and petrologic modeling of subduction zones: Geosphere, v. 16, no. 4, p. 936–952, https://doi.org /10.1130/GES02213.1.

Platt, J.P., 1986, Dynamics of orogenic wedges and the uplift of high-pressure metamorphic rocks: Geological Society of America Bulletin, v. 97, p. 1037–1053,

Raymond, L.A., 2017, What is Franciscan? Revisited: International Geology Review, v. 60, p, 1968– 2030.

Raymond, L.A., 2019, Perspectives on the roles of melanges in subduction accretionary complexes: A review: Gondwana Research, v. 74, p. 68–89.

Regalla, C.A., Rowe, C.D., Harrichhausen, N., Tarling, M.S., and Singh, J., 2018, Styles of underplating in the Marin Headlands terrane, Franciscan complex, California, in Byrne, T., Underwood, M.B., Fisher, D., McNeill, L., Saffer, D., Ujiie, K., and Yamaguchi, A., eds., Geology and tectonics of subduction zones: A tribute to Gaku Kimura: Geological Society of America Special Paper 534, p. 155–173.

Regional Water Quality Control Board, San Francisco Bay Region, 2004, Waste Discharge Requirements for Angel Island State Park.

Ring, U., 2008, Deformation and Exhumation at Convergent Margins: The Franciscan Subduction Complex: Geological Society of America Special Paper 445, 61 p., doi: 10.1130/2008.2445.

Sharman, G. R., Sharman, J. P., & Sylvester, Z. (2018). detritalpy: A python-based toolset for visualizing and analysing detrital geo-thermochronologic data. The Depositional Record, 4(2), 202–215.

Sloan, D, and Karachewski, J., 2006, *Geology of the San Francisco Bay Region*: California Natural History Guides, University of California Press, Berkeley, CA, 335 p.

Taliaferro, N.L., and Hudson, F.S, 1943, *Genesis of the Manganese Deposits of the Coast Ranges of California*, in *Manganese in California*: California State Division of Mines (CSDM) Bulletin No. 125, CSDM, Ferry Building, San Francisco, pp. 217-275.

Templeton, A.S., 2011, *Geomicrobiology of Iron in Extreme Environments*: Elements, v.7, pp. 95-100.

Tewksbury-Christle, C. M., Behr, W. M., & Helper, M. A. (2021). Tracking deep sediment underplating in a fossil subduction margin: Implications for interface rheology and mass and volatile recycling. Geochemistry, Geophysics, Geosystems, 22,

Trask, P.D., Wilson, I.F. and Simons, F.S.,1943, *Manganese Deposits of California: A Summary Report*, in *Manganese in California*: California State Division of Mines (CSDM) Bulletin No. 125, CSDM, Ferry Building, San Francisco, pp. 51-216.

United State Geological Survey, 2000. Is Seawater Intrusion Affecting Ground Water on Lopez Island, Washington? USGS Fact Sheet 057-00.

Wahrhaftig, C., 1984b1984a, Structure of the Marin Headlands Block, California: A progress report, in Blake, M.C., Jr., ed., Franciscan Geology of Northern California: Pacific Section, Society of Economic Paleontologists and Mineralogists (SEPM), v. 43, p. 31–50.

Wahrhaftig, C., 1984b, A streetcar to subduction and other plate tectonic trips by public transport in San Francisco (Revised ed.): Washington, D.C., American Geophysical Union, p. 76.

Wakabayashi, J. 2017, Structural context and variation of ocean plate stratigraphy, Franciscan Complex, California: insight into mélange origins and subduction-accretion processes: Prog Earth Planet Sci 4, 18. Wahrhaftig, C.,1984a. A streetcar to subduction and other plate tectonic trips by public transport in San Francisco. American Geophysical Union.

Wakabayashi, J., 2015, Anatomy of a subduction complex: Architecture of the Franciscan Complex, California, at multiple length and time scales: International Geology Review.